DUSTY PLASMA EFFECTS IN COMETS: EXPECTATIONS FOR ROSETTA

D.A. Mendis,[1] and M. Horányi [2]

Received 25 October 2012; revised 26 January 2013; accepted 31 January 2013.

[1] Despite their small masses, comets have played an extraordinary role in enhancing our understanding of cosmic physics. It was the calculation of comet Halley's orbit and the successful prediction of its return in 1758 that firmly established the correctness of Newton's law of universal gravitation. It was the morphology of the dusty tails of comets that provided the earliest information of the nature of the interaction of solar electromagnetic radiation with dust, and it was the orientation and structure of the plasma tails of comets that led to the discovery of the solar wind. More recently, the role of the changing dusty plasma environments of comets as natural space laboratories for the study of dust-plasma interactions, and their physical and dynamical consequences, has been recognized. The forthcoming Rosetta-Philae rendezvous and lander mission will provide a unique opportunity to revisit the entire range of earlier observations of dusty plasma phenomena in a single comet, as it moves around the Sun. In this topical review, motivated by the Rosetta mission, we discuss the varying modes of interaction of the comet as it approaches the Sun, and the different dusty plasma phenomena that are expected in each case, drawing on the earlier observations, including their interpretations and prevailing open questions.

Citation: Mendis, D.A., and M. Horányi (2013), Dusty plasma effects in comets: Expectations for Rosetta, *Rev. Geophys., 51*, doi: 10.1002/rog.20005.

1. INTRODUCTION

[2] Comets are among the smallest members of the solar system with typical masses $\approx 10^{-11} M_{\oplus}$. Yet they have played an extraordinary role in our understanding of cosmic and solar system physics. It was Edmund Halley's calculation of the orbit of a comet, now appropriately named after him, and the successful prediction of its return in 1758 that firmly established the correctness of Newton's law of universal gravitation, postulated in 1689. Comets, especially long-period comets, may be among the least metamorphosed and, consequently, the most pristine bodies in the solar system. It has also been proposed that they may have transported water and organic materials, essential to the evolution of life, during the early stages of development of our planet. While the heating of the "dirty ice" cometary nucleus is ultimately responsible for the overall activity of a comet as it approaches the Sun, paradoxically, it is the small size and negligible gravity of this nucleus that leads to its large atmosphere, dust tail, and plasma tail, which are typically 10^4 – 10^6 times larger than the dimension of the nucleus itself. It is noteworthy that the morphology of the dust and plasma tails of comets provided the earliest information of the nature of the interaction of solar electromagnetic radiation with dust and also led to the discovery of the continuous outflow of magnetized plasma from the Sun, which we now call the solar wind. The classical work of pioneers such as Friedrich Bessel and Fedor Brodikhin (dust tails), Ludwig Biermann and Hannes Alfvén (plasma tails), and the subsequent work in these areas by other authors, have been discussed in several comprehensive reviews [*Mendis et al*., 1985; *Mendis*, 2007].

[3] The importance of the dusty plasma environments of comets as natural space laboratories for the study of dust-plasma interactions, and their physical and dynamical consequences, has also been recognized. An important impetus to this area was provided by the ICE spacecraft fly-by through the tail of comet Giacobini-Zinner in 1985

[1]Department of Electrical and Computer Engineering, University of California, San Diego, La Jolla, California, USA.
[2]Colorado Center for Lunar Dust and Atmospheric Studies, Laboratory for Atmospheric and Space Physics, and Department of Physics, University of Colorado, Boulder, Colorado, USA.

Corresponding author: M. Horányi, Colorado Center for Lunar Dust and Atmospheric Studies, Laboratory for Atmospheric and Space Physics, and Department of Physics, University of Colorado, Boulder, Colorado 80309-0392, USA. (mihaly.horanyi@lasp.colorado.edu)

8755-1209/10.1002/rog.20005
Paper number 2012RG000422

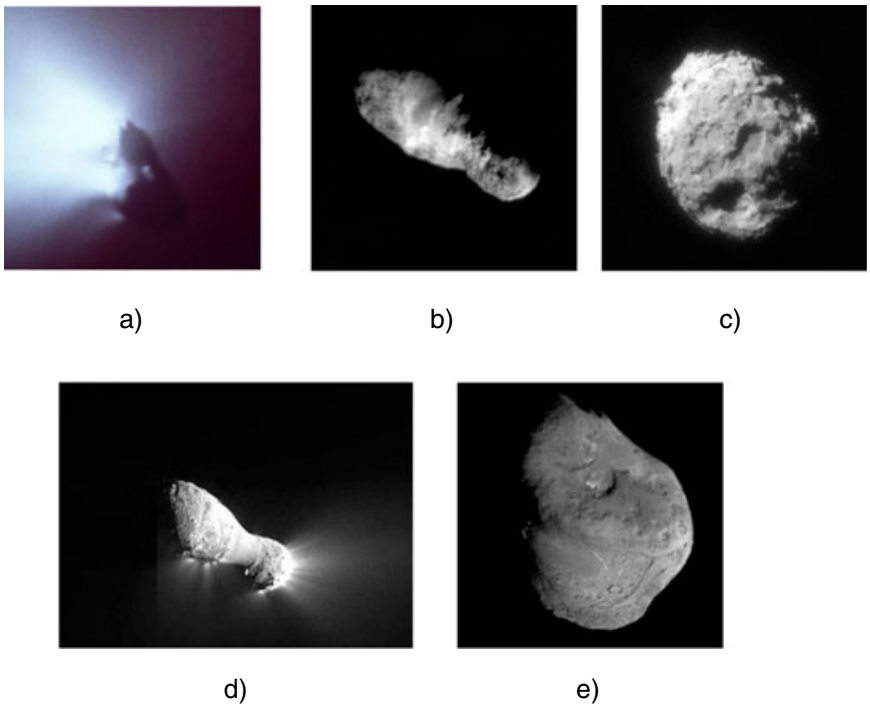

Figure 1. Five cometary nuclei have been imaged to date during close encounters by spacecraft: (a) 76P/Halley (Vega 1 and 2, Giotto, 1986); (b) 19P/Borelly (Deep Space 1, 2001); (c) 81P/Wild 2 (Stardust, 2004); (d) 103P/Hartley 2 (EPOXI, 2010); and (e) 9P/Tempel 1 (Deep Impact, 2004 and Stardust, 2011).

and the Vega 1 and 2, and Giotto spacecraft fly-bys (on the sunward side) of comet Halley in 1986 [*Mendis*, 1988; *Horányi and Mendis*, 1991]. Subsequent fly-by missions (Figure 1) have focused on the cometary nucleus and provided more details of the surface properties of four more comets [*Weaver*, 2004; *A'Hearn et al.*, 2005; *Brownlee et al.*, 2006; *Hartogh et al.*, 2011].

[4] In this topical review, our goal is to use the present understanding to anticipate the range of dusty plasma phenomena that would be observed during the ESA-Rosetta rendezvous mission to comet 67P/Churyumov-Gerasimenko in 2014. Unlike all the previous missions, which were fast fly-bys, the Rosetta mission, which was launched in March 2004, and will encounter the comet in mid 2014, will deploy its surface lander (Philae) in November of 2014, and escort the comet around the Sun, until the end of its nominal mission in December 2015. Consequently with its large complement of instruments, we expect this mission to observe the entire range of dusty plasma phenomena observed earlier (both by spacecraft fly-bys and ground-based and Earth orbiting observatories) in different comets, at different heliocentric distances. It is expected that these observations would be at higher resolutions and be more detailed, and thereby provide a deeper understanding of the phenomena. Also, the Philae lander would provide high resolution, in situ data on the nucleus, and perhaps show, charge-induced dust migration on the surface. It is our hope, that in addition, novel dusty plasma phenomena may also be discovered.

[5] This review is organized as follows: we start with a brief overview of the basic physics of dusty plasmas in space including the central issue of grain charging and the associated physical and dynamical consequences for both the dust and the plasma (section 2). This is followed, (in section 3) with a description of varying particles and fields environment of a comet as it approaches the Sun. In the following sections (4–7) we discuss several classes of cometary phenomena that have been attributed to dust-plasma interactions, namely electrostatic levitation and blow-off of charged dust from the cometary nucleus (section 4), electrostatic disruption of charged dust (section 5), consequences for the overall spatial distribution of fine dust in both the head and tail of comets (section 6), and the rapid changes in the dust tail morphology during the crossing of magnetic sector boundaries in the solar wind (section 7). The proposal for the possible role of dust in the formation of the inner shock within the cometary ionopause is discussed in section 8. In section 9, we provide a brief description of the Rosetta-Philae, rendezvous-lander mission to comet 67P/Churyumov-Gerasimenko in 2014, with emphasis of the main instruments that would contribute to the study of dusty plasma phenomena at the comet. We conclude (section 10) with a summary of the expected contribution of the mission to our understanding of dusty plasma phenomena at comets over a range of qualitatively different cometary environments, defined by the varying nature of the interaction of the solar wind and solar radiation with the comet as it approaches the Sun.

2. BASIC PHYSICS OF DUSTY PLASMAS: GRAIN CHARGING AND ITS PHYSICAL AND DYNAMICAL EFFECTS

[6] After a slow start, the physics of dusty plasmas, which have now been observed not only in its usual gaseous phase but also in its liquid and solid phases, and exhibiting novel wave modes and instabilities, is presently in a rapid state of development. There are several useful review papers [*Goertz*, 1989; *Mendis and Rosenberg*, 1994; *Horányi*, 1996; *Horányi et al*., 2004] and textbooks [*Verheest*, 2000; *Shukla and Mamun*, 2002; *Bliokh et al*., 1995; *Tsytovich et al*., 2008] available on the study of solar system and cosmic dusty plasmas. In this section, we provide a quick overview of the basic dusty plasma physics relevant to the phenomena at comets to be discussed in the subsequent sections.

[7] Central to this study is the electrostatic charging of grains (in isolation or in an ensemble) in plasma and radiative environments. This is given by

$$\frac{\mathrm{d}Q}{\mathrm{d}t} = \frac{\mathrm{d}}{\mathrm{d}t}\left(C(\phi - \bar{\phi})\right) = I_{\mathrm{tot}}, \tag{1}$$

where Q is the grain charge, C is the grain capacitance, ϕ and $\bar{\phi}$ are the grain surface potential, and the average ambient plasma potential, respectively. Contributions to the total current reaching the grain's surface, I_{tot}, can come from processes, including background electron and ion collection, secondary electron emission (due to energetic electron or ion impact), thermionic emission (due to grain heating), photoelectron emission, field emission of electrons (due to large surface fields), etc. [*Whipple*, 1981; *Mendis*, 2002]. These currents depend on the properties of both the grains and the ambient plasmas.

[8] For example, the electron and ion collection currents depend on the size and electrical properties of the grain, the electron and ion densities, n_e, n_i, respectively, and the composition of the plasma, the velocity distributions of the electrons and ions, and the motion of the grain through the plasma. They can also depend on the spatial density distribution of the dust particles. The simplest case corresponds to an isolated grain where both the radius of the grain, a, and the characteristic distance between the grains, d, is much smaller than the characteristic shielding distance of their plasma environment, $\lambda_D = (k_B T/4\pi n_p e^2)^{1/2}$. In this case, $a \ll \lambda_D \ll d$, and the capacitance is $C = a(1 + a/\lambda_D) \simeq a$, and $\bar{\phi} = 0$. For a Maxwellian electron and ion distribution with equal temperatures of $T_e = T_i = T$ with stationary dust particles, the so called orbit limited currents can be readily calculated and the equilibrium potential of the grain, ϕ_{eq} can estimated by setting $I_{\mathrm{tot}} = 0$ in equation (1).

[9] In the absence of UV radiation, in a plasma with $n_e = n_i$, and $T_e = T_i = T$, equation (1) yields $\phi_{\mathrm{eq}} = -\alpha k_B T/e$, where α is increasing logarithmically with ion mass, for example, with values of 2.5 and 3.6, for hydrogen and oxygen plasmas, respectively. The reason for the negative values of ϕ_{eq} is the higher mobility of the electrons vis-á-vis the heavier ions, which requires a negative grain potential, to retard the inflowing electrons and accelerate the inflowing ions to equalize the two currents at equilibrium.

[10] The case where there are many grains within a Debye sphere (i.e., $a \ll d \ll \lambda_D$) in an isothermal Maxwellian plasma, has also been considered [*Goertz and Ip*, 1984; *Whipple et al*., 1985; *Havnes et al*., 1987] and verified in the laboratory [*Xu et al*., 1993; *Bouchoule and Boufendi*, 1993]. In this case too, grains acquire a negative charge, which is however (numerically) smaller. This is due to the depletion of electrons required by the charge neutrality conditions: $n_e + n_i + zn_d = 0$, which in this case can result in $n_e \ll n_i$, so $\phi_{\mathrm{eq}} - \bar{\phi}$ needs not be as negative as in the case of the isolated grain, for the grain charging currents to be equal at equilibrium. Therefore, $|Q| = C|\phi - \bar{\phi}|$ decreases despite a slight increase in C [*Whipple et al*., 1985]. The electron depletion cannot be complete, as it has sometimes been assumed in the literature, because in that case, there could be no electron current to balance the finite ion current to the grains to have a steady state charge. The apparent inequality between the ion and electron densities due to the presence of dust has been observed by rocket measurements in the Earth's mesosphere [*Reid*, 1990] and, more recently, in the active plumes of Saturn's moon Enceladus by Cassini [*Morooka et al*., 2011].

[11] So far, it has been implicitly assumed that the grain charging process is a continuous one, and that all grains achieve the same equilibrium potential, hence acquire a number of extra/missing electrons $|Q_e/e| \approx 700 a_\mu |(\phi - \bar{\phi})|$, where the radius of the grain is measured in μm. This is legitimate for sufficiently large grains. For example, a micrometer-sized grain in an isothermal hydrogen plasma with $k_B T = 3$ eV, has ≈ 5000 excess electrons on its surface. On the other hand, a nanometer-sized grain, in the same plasma carries, on the average, an excess of only five electrons. Consequently, the stochastic nature of their charging, which leads to significant fluctuations, has to be taken into account. This stochastic process can be simulated by a Monte Carlo approach [*Cui and Goree*, 1994] or analytically as a one-step Markov process [*Matsoukas and Russell*, 1995]. In either case, what is obtained is the charge distribution function, $f(z)$, which is the probability of finding the grain in the charge state, z.

[12] Other processes of grain charging, such as photoelectric emission, thermionic emission, etc., would lead to the grain being positively charged, should they be the dominant charging process. Perhaps the most interesting of these charging processes is secondary electron emission from the grain due to energetic electron impact in a hot plasma. Calculation of current-voltage curve shows it to have multiple roots, due to the shape of the secondary electron yield (i.e., the number of secondary electrons emitted by the grain per incident electron), which first increases with energy to a maximum that could be greater than unity and then decreases [*Whipple*, 1981]. The consequence of grains in a plasma acquiring charges of opposite polarity during transient variations of temperature, have been discussed [*Meyer-Vernet*, 1982; Horányi and Goertz, 1990], and its validity has also been established in the laboratory

[*Walch et al*., 1995]. Another interesting property pertaining to secondary electron emission by electron impact is that even in the absence of such transient effects, grains of different sizes can acquire different polarities, with the smaller ones being positive and the larger ones being negative. This is due to the fact that, when the grain size becomes comparable to the penetration depth of the primary electrons, the secondary electron emission yield increases sharply [*Chow et al*., 1993; *Watanabe*, 1997].

[13] High concentration of dust can lead to electron depletion in a thermal plasma, when the dominant charging currents are due to electron and ion collection. Alternately, dust grains can also lead to an increase of the electron density in a plasma, when photoelectron emission, thermionic emission of electrons, electric field emission and secondary emission are dominant [*Mendis*, 2002]. Sputtered ions can change the composition of the plasma environment.

[14] The charging of grains in a plasma can lead to physical and dynamical consequences for the dust. We discuss these in subsequent sections, as they apply to the changing cometary environment. The physical consequences include electrostatic levitation and blow-off of dust from the charged cometary nucleus and electrostatic disruption and erosion of charge dust in the cometary plasma environment. The dynamical consequence arises from the new electrodynamic forces that charged dust grains experience in the magnetized plasma environment of the comet.

3. THE VARYING PARTICLES AND FIELDS ENVIRONMENT OF A COMET ORBITING THE SUN

[15] As the Rosetta spacecraft (together with its Philae Lander) encounters comet 67P/Churyumov-Gerasimenko at a heliocentric distance of about 4 AU and escorts it through perihelion (at 1.29 AU) and beyond, it will encounter a wide range of particles and field environments, which differ not just quantitatively, but qualitatively as well. Since the anticipated cometary dusty plasma phenomena that is discussed in subsequent sections will occur in this highly variable environment. The varying modes of interaction of the solar wind and solar radiation, with comets, as they orbit the Sun, in their elliptical orbits, have been discussed, in detail elsewhere [*Mendis et al*., 1985; *Flammer*, 1988, 1991; *Flammer et al*., 1992; *Mendis*, 2007; *Coates and Jones*, 2009]. Here, we confine ourselves to a brief overview, sufficient for the purposes of this review. Central to the following discussion is the ultimate source of all observed cometary activity, its nucleus.

3.1. The Nucleus

[16] Although not resolved by ground-based observations, the existence of a discrete, cohesive nucleus composed of volatile ices (e.g., H_2O, CO_2, CO, NH_3, CH_4, etc.) and non-volatile (meteoritic) dust was widely accepted, since it was proposed by *Whipple* [1950] in a seminal paper. Since then, this model, with essential modifications over time, has been the basis of all subsequent work on the dynamics, physics, and chemistry of comets. These essential modifications had to do with the nature of the ices, the possible formation of nonvolatile mantles (already anticipated by Whipple) due to incomplete entrainment of the surface dust by outflowing gases, as well as the layering of sub-surface ices (with the least volatile H_2O ice, closest to the surface, and the more volatile ices, further down) due to chemical differentiation caused by thermal processing [*Mendis et al*., 1985].

[17] Since 1986, spacecrafts have encountered and imaged the nuclei of five periodic comets, which are shown in Figure 1. It is apparent that these small bodies have irregular shapes, with comet 81P Wild 2 (Figure 1c) being closest to sphericity. A striking aspect of all these bodies is their darkness, with geometric albedos of only a few percent. All these cometary nuclei were imaged when they were sufficiently close to the Sun (from d = 0.83 AU for Halley, to d = 1.8 AU for Wild 2) to be strongly outgassing. In the case of comet Halley, the outgassing rate was $\sim 10^{29}$ mol/s, over 80% of which was H_2O and about 10–15% of CO [*Mendis*, 1988]. While the outflow of H_2O and other gases from the nucleus is not observed visually, the dust that is entrained by outflowing gas acts as a tracer. It is clearly seen in the case of comet Halley (Figure 1a) that the dust is not flowing out isotropically, but rather in the form of highly localized sunward jets. While too faint to be seen in the images of the other comets, excepting comet Hartly 2 (Figure 1*d*), the dust emission from them are also largely in the form of sunward jets, localized to small fractions of their surfaces.

[18] These observations lead to the inferences of a non-uniform inactive crust overlying a volatile mix of subsurface ices (presumably, mainly H_2O) and non-volatile dust. The thickness, porosity, and friability of this outer crust could be highly variable, and it may also have fissures. In such a case, the outgassing would preferentially be from the regions of low crustal thickness, high porosity, or fissuring. Such regions of structural weakness may also be the regions from which dust could be more easily entrained by the outflowing gases. General support for a fragile dust layer, overlying an H_2O-ice dominated interior, was provided by the *Deep Impact* mission, which launched the projectile from the spacecraft onto the surface of comet Tempel 1 on 4 July 2005 [*A'Hearn et al*., 2005]. Much more detailed data on the structure and composition of the cometary surface is expected from the Rosetta mission, which includes the Philae Lander.

3.2. Comet Solar Wind Interaction

[19] In considering the varying nature of the interaction of a comet with solar radiation and the solar wind, it may seem natural to begin with the time when the nucleus is sufficiently far from the Sun, when it is still inactive and follow it as it moves sunward, sprouting a fledgling atmosphere, which grows steadily in size and density, as the comet approaches perihelion. Here, we discuss it in reverse, starting with the time when the comet has a well-developed atmosphere. This is because the nature of the comet-solar wind interaction has been studied, most extensively, in this mode, as was the case with the multi-spacecraft encounters of comet Halley, in the spring of 1986

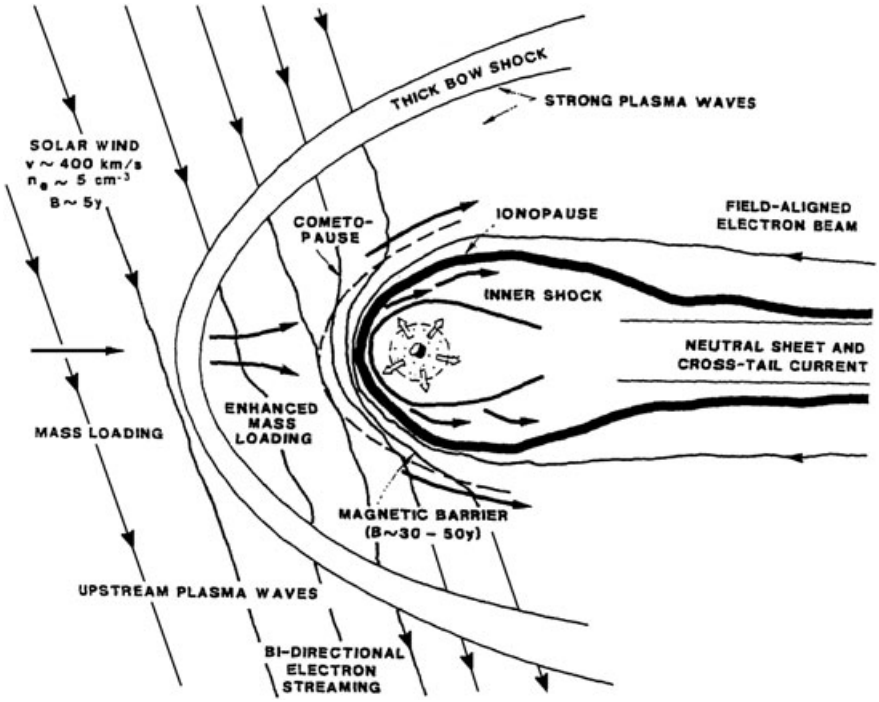

Figure 2. The particles and fields environment of an actively outgassing comet [*Mendis*, 1988].

following the ICE spacecraft fly-through of the tail of comet Giacobini-Zinner in the fall of 1985. Figure 2 shows the schematics of the global morphology of the interaction of two supersonic flows.

[20] As the supersonic (and super-Alfvénic) magnetized solar wind flows towards the comet, it picks up heavy cometary ions such as O^+ (which are produced by photoionization by solar UV radiation or by charge exchange with solar wind protons). The consequent mass-loading slows down the inflowing solar wind which eventually undergoes a week ($M \approx 2$) shock, upstream of the nucleus, typically around a distance of $(10^4 - 10^5)R_n$ from it, when it has picked up only a few percent of the cometary ions. Incidentally, the distance of the shock from the nucleus is somewhat larger when the shock is quasi-perpendicular than when it is quasi-parallel [*Flammer*,1991].

[21] The inflowing, sub-sonic solar wind continues to slow down while its magnetic field continues to increase, and is eventually brought to stagnation (along the Sun-comet axis) and diverted around the cometary ionosphere by a tangential discontinuity surface, loosely referred to as the ionopause. The basic mechanism responsible for the formation of this ionopause appears to be essentially the balance between the electromagnetic $\mathbf{j} \times \mathbf{B}$ force and the drag of the outflowing cometary neutrals on the plasma just outside it.

[22] The supersonically outflowing cometary ionosphere, within the ionopause, results from the photoionization of the cometary neutral species (e.g., O^+, OH^+, H^+, CO^+, etc.) by solar UV radiation, followed by the reshuffling of these ions, by ion-neutral reactions within this dense, collisionally dominated region. The neutrals sublimate from the nucleus, which is heated by solar radiation. Since the gravity of the cometary nucleus is negligible, these neutrals expand freely outward, entraining fine cometary dust. While the drag of the neutrals accelerate the dust to a terminal speed within a few tens of cometary radii, the reverse drag of the dust on the gas plays the role of a De Laval nozzle making the flow transonic near the nucleus. Since the photoions, within the ionosphere, are collisionally coupled to the supersonically outflowing neutrals within the ionosphere, they must undergo a shock within the ionopause (Figure 2), while the neutrals, which are unaffected by the magnetic field, flow out unimpeded. The nature of this shock and the possible role of charged dust, on its formation, is discussed in section 8.

[23] The basic correctness, both qualitatively and quantitatively, of the comet-solar wind interaction model (Figure 2), which is based on theoretical predictions was verified by the multi-spacecraft mission to Halley's Comet in 1986, the ICE spacecraft mission to comet Giacobini-Zinner, in 1985, and the Giotto spacecraft to comet P/Grigg-Skjellerup [*Mendis*, 1988; *Flammer*, 1991; *Flammer et al*., 1993]. The sizes of the various flow regimes delineated by the discontinuities in the flow (e.g., the outer shock, the ionopause, and the inner shock) depend crucially on the production rate of gas (mainly H_2O) from the nucleus, which in turn depends on the amount of solar radiation absorbed by it. Consequently, as the comet moves away from the Sun, all of these regions shrink in size and may eventually collapse and cease to exist. For instance, in the case of comet Halley, (production rate $Q \simeq 6.9 \times 10^{29}$ mol/s, at $d = 0.89$ AU) Q becomes sufficiently small, when $d \geq 2.2$ AU, that the outflowing neutrals do not possess enough momentum to stand-off the solar wind upstream of the nucleus. Yet the mass-loading of the inflowing solar wind, is sufficient to produce a weak shock upstream.

[24] Consequently, the solar wind, having turned subsonic at this shock, flows all the way to the nuclear surface. Hence, a magnetic field-free ionosphere surrounding the nucleus no longer exists. As this comet moves still further away from the Sun, the mass loading of the inflowing solar wind becomes insufficient to produce this shock. In this situation, the slightly contaminated and unshocked solar wind flows supersonically on to the unprotected nucleus [*Flammer et al*., 1992]. Interestingly, *Brandt* [1987] suggested that the time when one begins to observe a fledgling plasma tail is when the comet has formed a well-developed ionopause. Calculations showed that this would be the case for comet Halley (in 1986) when its heliocentric distance was $\approx$ 2.2 AU [*Flammer and Mendis*, 1991], as discussed above. Observation of the turn-on time of the plasma tail, for this comet, was at $d \approx 1.8$ AU (inbound), while the corresponding turn-off time was at $d \approx 2.3$ AU (outbound). These observations are deemed to be in a reasonable agreement with the predictions, considering the inherent large uncertainties in the solar wind conditions and in the parameters of the theoretical models [*Brandt*, 1990]. These models could be verified and improved during the Rosetta mission.

[25] The foregoing discussion of the comet-solar wind interaction is based on a single-fluid model of the magnetized solar wind. The validity of this model was questioned early on by *Wallis and Ong* [1975] on the grounds that the newly created cometary ions do not quickly accommodate to the solar wind flow, thus needing the use of a kinetic approach to describe their dynamics. Subsequently several authors used a kinetic equation for the picked-up cometary ions to discuss certain aspects of this interaction, such as the nature of the outer bow shock [*Galeev*, 1987]. Also, *Flammer et al*. [1992] developed a self-consistent model for the particles and fields upstream of an outgassing comet, in order to study the global interaction of the solar wind with the tenuous atmosphere of the comet, when far from the Sun. This study was motivated by the defunct NASA-CRAF mission to a comet, which was very similar in its conception to the Rosetta mission. This model, which starts with the velocity distribution of the cometary pick-up ions, and their time evolution, would be applicable to the solar wind interaction with comet 67P/Churyumov-Gerasimenko during the earlier stages of the Rosetta encounter with it.

[26] In the absence of an ionopause, the mass-loaded solar wind would flow unimpeded on to the cometary nucleus either supersonically (further away from the Sun) or subsonically (closer in to the Sun). In either case, the associated plasma currents, together with the photoemission current produced by the attenuated solar UV radiation, would lead to differential charging of the sunward side of the cometary nucleus. In the absence of a cometary ion tail, which may presumably be the case, and in the absence of an ionopause, the shadowed side of the cometary nucleus could charge up to large negative potentials, due to the buildup of a negative space charge, as the solar wind blows past, as discussed in section 4.

[27] There, we have also considered the consequence of this surface charging for loose, fine cometary dust lying on the surface (electrostatic levitation) and discussed it in connection with certain dust observations for Halley's comet, during its 1986 apparition. Admittedly, the observations of Halley's comet occurred when the comet was far from the Sun and it was not, or only weekly, outgassing. The comet 67P/Churyumov-Gerasimenko is expected to be only weakly outgassing when the Rosetta spacecraft first encounters it at around 4 AU from the Sun. Yet this outgassing would be insufficient to prevent the slightly mass-loaded solar wind from flowing supersonically on to the nuclear surface. In the expected absence of a plasma tail, there could also be a buildup of solar wind associated, negative space charge behind the nucleus. So the early stages of the encounter may provide an opportunity to verify if the levitation of charged dust above the nuclear surface, as discussed in section 4, does in fact take place.

[28] In order to calculate the heliocentric distances at which the solar wind interaction with a comet changes its nature, as discussed above, one needs to estimate the variation of the production rate of the cometary volatiles (or at least that of the dominant one), with heliocentric distance, in the first instance. This requires the solution of the quasi-steady state, energy balance equation on the cometary surface, which equates the total amount of solar energy absorbed by the surface to that used for the heating (and subsequent re-radiation by the heated surface) together with that used for the sublimation of the heated volatiles. For this purpose one needs to know the physical properties of the nucleus (e.g., size, geometric albedo, and structure) as well as the chemical composition of the volatile component. The latter leads to the appropriate Clapeyron-Clausius equation for the sublimation rate for the volatile species in question.

[29] A proper calculation also requires a knowledge of the optically significant dust halo surrounding the nucleus, since this participates in the radiative transfer of radiation to and from the surface. Since the amount of dust itself results from the rate of outflow of the volatiles, a self-consistent model for the production rate of the volatiles is not a trivial problem [*Mendis et al*., 1985]. Typically, one is forced to make several simplifying assumptions. This includes the adoption of a uniform average surface temperature (justifiable if the rotation rate is sufficiently fast) and that the sublimation rate is controlled by the predominant volatile molecule in the nucleus (H_2O). In this case, one gets a profile for $\dot{z}(d)$ (the flux of H_2O molecules) with a characteristic shape, exhibiting a sharp knee at a heliocentric distance (d) of about 3 AU (which depends somewhat weakly on the assumed surface albedo).

[30] The reason for this knee is the following: when the comet is at a distance $d > 3$ AU, the energy balance at the surface is determined largely by the absorption of solar radiation and the re-radiation from the heated surface, because the temperature is too low to produce significant sublimation. So, the surface temperature rises rapidly as the comet approaches the Sun, leading to a rapid increase in the (albeit small) production rate of H_2O. When $d \approx 3$ AU, the surface temperature becomes large enough to produce sufficient H_2O sublimation, that most of the absorbed solar heat now

goes into the energy of sublimation. So when $d \leq 3$ AU, the rate of heating of the nucleus decreases with d, leading to a slower increase of the production rate of H_2O as d decreases. Hence the knee.

[31] The total production rate of H_2O from the comet, $\dot{Q} = 4\pi R_n^2 \dot{z} f$, where R_n is the effective spherical radius of the irregularly shaped nucleus, and f is the fraction of the surface that is active (e.g., where the porosity or the fissuring is high; see earlier discussion). For Halley's Comet $R_n \approx 4.5$ km, and $f \approx 10\%$. Comet 67P/Churyumov-Gerasimenko seems to be smaller than comet Halley, with $R_n \simeq 1.7$ km, and f estimated to be $\simeq 4\%$, from ground-based observations [*Combi et al*., 2012a; b].

[32] Besides $\dot{Q}(d)$, one also needs working models of the solar wind, and the interplanetary magnetic field, during the period of encounter of the comet by Rosetta (2014–2015), in order to make reliable estimates of the heliocentric distances at which the outer shock and the ionopause would appear, as discussed earlier in connection with comet Halley. Nevertheless, it is possible to make an estimate of the size of the outer bow shock and the ionopause of comet 67P/Churyumov-Gerasimenko, at least near its perihelion, from what is already known.

[33] During its last perihelion passage (at $\simeq 1.27$ AU) a gas production rate of $Q \simeq 2 \times 10^{27}$ mols/s was estimated [*de Almeida et al*., 2009]. The predicted perihelion distance at the next apparition is $\simeq 1.29$ AU. So Q could be somewhat smaller. Based on the model by *Flammer* [1991], and assuming the previously observed value of Q, the location of the bow shock along the sun-comet axis is expected to be at a distance of $R_S \simeq 3.2 \times 10^4$ km and $R_S \simeq 1.8 \times 10^4$ km, for the quasi-perpendicular and quasi-parallel shocks, respectively. For typical solar wind conditions the expected value of R_S is much larger than the Larmor radius, $L_C \sim 100$ km, of a cometary pickup ion (e.g., O^+), hence, the shock is expected to be well defined.

[34] For the same assumptions [*Flammer*, 1991], the location of the ionopause along the sun-comet axis, is predicted at $R_C \simeq 95$ km . The criterion for the ionopause to be well defined is that $R_C \gg L_i$, where L_i is the Larmor radius of a solar wind ion in the contaminated subsonic solar wind flow just outside the location of the ionopause. For conditions similar to Halley's comet, the magnetic field just outside R_C is $B_i \simeq 40$ nT, resulting in a Larmor radius of $L_i(H^+) \simeq 10$ km, and $L_i(O^+) \simeq 40$ km, barely satisfying the criterion for a well defined ionopause.

[35] Yet, another problem is that an ionopause with such a small radius of curvature maybe subject to the 'flute' instability [*Ip and Mendis*, 1978]. Consequently, it is not clear that a well-defined ionopause, bounding a magnetic field-free cavity, would form in this comet even at perihelion. A similar situation existed when the Giotto spacecraft flew-by comet P/Grigg-Skjellerup in 1992, showing a production rate of $Q \simeq 7 \times 10^{27}$ mols/s at a heliocentric distance of 1.1 AU. Unfortunately, the closest fly-by distance was larger than the estimated size of R_C. Thus, it was not possible to verify the existence or non-existence of magnetic field-free cavity [*Flammer and Mendis*, 1993]. We expect that during the Rosetta mission, the formation, or the lack of, a diamagnetic cavity near a weekly-outgassing comet will be verified.

4. ELECTROSTATIC LEVITATION OF CHARGED DUST ON THE COMETARY SURFACE

[36] When a surface containing loose dust grains is electrically charged, the charged grains experience an electric force due to the electrostatic field generated on the charged surface. This could include a force repelling the grain away from the surface, due to the normal component of the surface electric field as well as force along the surface due to the component of the electric field parallel to the surface. If this normal electrostatic force on the grain is large enough to overcome the normal force (cohesive or gravitation) pulling it toward the surface, the grain can be lifted off the surface. If the tangential electrostatic force on the grain is large enough to overcome the surface forces (cohesive or frictional) that tend to prevent its motion on the surface, it will be transported on it. While this process has been observed and studied in the terrestrial laboratory [*Sheridan et al*., 1992; *Sickafoose et al*., 2002; *Flanagan and Goree*, 2006; *Wang et al*., 2009], several observed solar system phenomena on the Moon, planetary rings, asteroids and comets, that inspired these experiments, still presents many open questions. Theoretical models of dust dynamics in plasma and UV sheath are also available [*Nitter and Havnes*, 1992; *Mitchell et al*., 2006; *Poppe and Horányi*, 2010], although the mechanisms for the initial mobilization of charged grains still presents unresolved questions. Here, we confine ourselves to the case of comets.

[37] When a comet is sufficiently far from the Sun, its outgassing rate is low, and consequently its resulting atmosphere is too thin to impede the inflow of the solar wind or to attenuate the solar UV radiation to its surface. The heliocentric distance beyond which this happens depends crucially on the chemical composition of the volatile ices that constitute the dirty ice cometary nucleus, as well as its size and structure. Assuming the cometary nucleus to be a water ice dominated sphere with loose dust on its surface, *Mendis et al*. [1981] calculated its differential charging at various heliocentric distances, using two different models of the solar wind. The charging currents included were the electron and ion collection currents and the photoelectric emission currents due to the solar ultraviolet radiation. Assuming the surface to be a good insulator, they used the current balance at each point on it to calculate the local electrostatic potential, as was done for the sunlit lunar surface [*Manka*, 1973]. Details aside, the basic result was that, for the entire range of heliocentric distance ($d > 5$ AU) considered, the surface potential varied from small positive values ($\phi \approx 5$ V) near the subsolar point to, numerically, moderately large negative values near the terminator ($\phi \approx -10$ to -20 V). The reason for this is the very rapid decrease of UV radiation with increasing angle of incidence.

[38] With essentially a Debye potential, at the surface, the normal component of the surface electric field, $E_n \approx \phi_s/\lambda_D$,

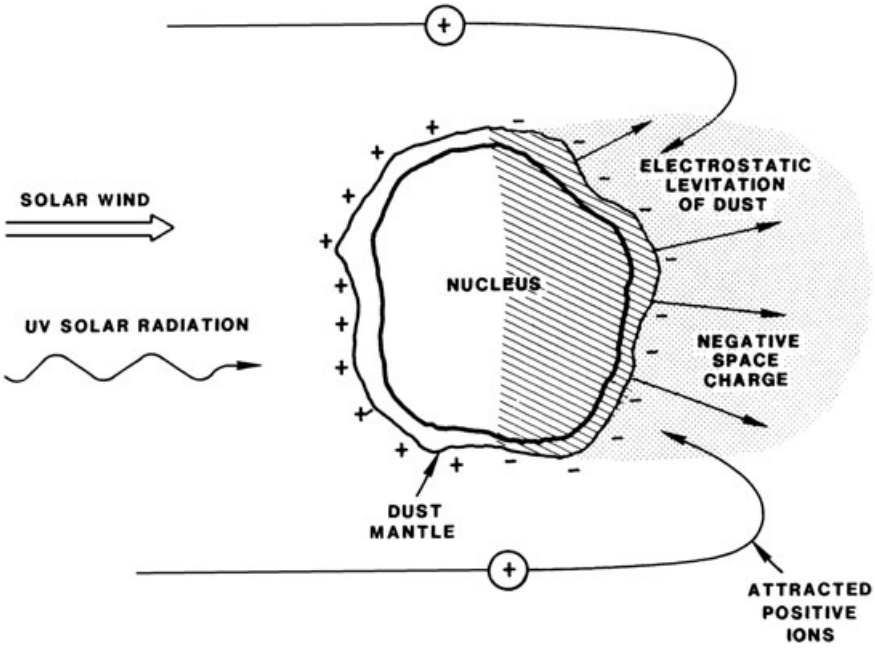

Figure 3. Schematic drawing of the basic model to estimate the electrostatic potential acquired by the night side of an unshielded cometary nucleus.

where λ_D is the usual plasma Debye shielding length. Over most of the surface, where ϕ_s is positive, λ_D is the characteristic thickness of the photoelectron sheath. In reality, there is also a component of the electric field, E_t, tangential to the meridian. However it is expected to be much smaller as the normal component, since $E_t = \frac{1}{R_N}\frac{d\phi_s}{d\theta} \ll E_n$ (except very near the terminator), where R_N is the radius of the nucleus. The terminator region, where sharp lit-dark boundaries exist, might exhibit regions where $E_n \simeq E_t$ [*Wang et al*., 2007]. A dust grain, with radius a, lying on a surface with a surface charge density σ acquires a charge Q, that is proportional to its projected surface area, as was first pointed out by *Singer and Walker* [1962]. Using Gauss' law, $Q = \pi a^2\sigma = a^2E_n/4 = a^2\phi_s/(4\lambda_D)$. Since $\lambda_D \gg 1$ m, and $Q \approx (a\phi_s)(a/4\lambda_D) \ll Q_{isolated}$, the charge on a grain lying on the surface is much smaller than what it would acquire as an isolated grain off the surface.

[39] *Mendis et al*. [1981] found that grains in the size range 0.1–10 μm have an excess charge of $N = Q/e \ll 1$. Since a grain cannot carry a fractional charge, they interpreted this to mean that only a fraction, N, of the grains would carry a unit charge, and concluded that such grains could overcome the gravitational attraction of the nucleus if $a \leq 0.3\mu$m, typically. Since such grains can acquire more extra charges, corresponding to their free-space value, once they are lifted off the surface, they can acquire enough energy to be eventually blown off the surface. Calculating the surface potential on the night side of the comet was not straightforward, but the above authors argued that it must be numerically large and negative. This follows from the fact that, while the solar wind is supersonic with respect to the ions, it is subsonic with respect to the electrons. This leads to a depletion of the ions and a consequent build up of negative space charge in the wake, leading in turn, to a numerically large, negative surface potential. They expected that this surface potential to keep increasing numerically, until it was large enough to deflect the solar wind protons moving past the comet with kinetic energy $E_k = 1/2m_pv_{sw}^2$, which results in a nightside surface potential of $\phi_s \approx m_pv_{sw}^2/(2e)$ (Figure 3). This led to $\phi_s \approx -550$ V in the slow solar wind ($v_{sw} \approx 330$ km/s) and $\phi_s \approx -2550$ V in the fast solar wind ($v_{sw} \approx 700$ km/s). Assuming, the uncertain value of the plasma Debye length λ_D on the night side of the comet to be $\approx R_N$ (the radius of the nucleus), the authors found grains of radii about 0.5 μm could be blown off the night-side surface when the solar wind was slow, while this value increased to about 1 μm when the solar wind was fast.

[40] *Flammer et al*. [1986] used the above mechanism of solar wind modulated dust levitation and blow-off of charged dust from the dark side of the comet, to explain the sporadic variations of the brightness of comet Halley (by as much as 500%) at large heliocentric distances 11.8 AU, (inbound), when the comet was not outgassing. These authors also showed that the comet encountered a corotating, high-speed solar wind stream, emanating from a southern coronal hole, at the times of the observed brightness increases. Subsequently [*Intriligator and Dryer*, 1991], attributed a large brightness increase of comet Halley at 14.3 AU (outbound) to its interaction of a solar flare generated shock wave moving at a high speed of 750 km/s. While these authors suggested that the outburst resulted from dust released from the pressure-induced rupture of the nucleus, *Mendis and Rosenberg* [1994] argued that this was unlikely because the ram pressure of this fast solar wind at 14.3 AU was estimated to be only $\approx 3\times10^{10}$ N/m^2, which was far too small for the purpose. They suggested, instead, that physical

process responsible for the dust emission was the electrostatic dust levitation and blow-off from the dark side of the comet, as discussed earlier.

[41] The Rosetta-Philae mission to comet 67P/Churyumov-Gerasimenko during its early encounter (around 4 AU) could provide us with an opportunity to check the validity of the *Mendis et al*. [1981] model for the levitation and blow-off of charged dust from the night side of the comet, with high-resolution observations of the near-surface environment of the comet. The existing support for this model is provided by the ground-based observations of distant comets. Also, while there are some measurements of numerically large negative potentials ($\approx$ 1 kV) on shadowed areas of spacecraft [*Whipple*, 1981; *Davis et al*., 2008], it will be important to see whether such potentials are indeed achieved on the night side of the comet. High-resolution observations of charged dust transport on and near the cometary surface could also shed light on processes that have been proposed to occur on other atmosphereless bodies in space, such as, for instance, the ill-understood super charging process at the boundary of shaded and sunlit areas on the Moon [*Criswell and De*, 1977; *Wang et al*., 2007].

5. ELECTROSTATIC DISRUPTION IN THE COMETARY ENVIRONMENT

[42] When a body is electrically charged, the mutual repulsion of the surface charges lead to an electrostatic tension. If the total electrostatic force across any plane section of the body (which may be calculated by integrating the component of this electrostatic tension, normal to the plane section over either part of the body, bisected by the plane) exceeds the total tensile force across the plane section, the body will be electrostatically disrupted across that section. It was shown by *Öpik* [1956], that a uniformly conducting spherical solid of radius a and surface potential ϕ and of uniform tensile strength F_t would be split in half if the electrostatic tension $F_E = \epsilon_0 E^2/2 \simeq \phi^2/(2a^2) > F_t$. This implies that in order to escape disruption, the radius of a dust grain must exceed a critical value $a_c(\mu\text{m}) \simeq 20 \times F_t^{-1/2} |\phi(\text{V})|$. Incidentally, electrostatic disruption of spherical liquid droplets and bubbles had been discussed much earlier by Lord Rayleigh (1882), for the case of the cohesive force provided by surface tension. Noting that cosmic dust grains are expected to be far from spherical, *Hill and Mendis* [1981] discussed the electrostatic disruption of non-spherical, conducting grains idealizing them as prolate spheroids. These authors showed that as such a body (assumed to be of uniform tensile strength) is charged up, it will begin to electrostatically chip-off at the poles, since that is where the electric field (and hence the electrostatic tension) would be largest. As the grain potential increases, this electrostatic chipping will continue with the grain becoming more spherical. This chipping process will eventually cease, while the grain is still prolate, if its tensile strength is large enough. If not, the process will continue until the grain becomes more or less spherical, at which point it would split in two. Since the electric tension is greatest at points where the radius of curvature is smallest, the authors drew the obvious conclusion that, if the surface of a conducting body of uniform tensile strength were irregular, these irregularities would be eroded, with the body becoming progressively smoother as the body was charged up. While to the best of our knowledge, there are no laboratory observations of electrostatic disruption of charged dust grains, a very interesting recent development concerns its possible role in the sterilization of biological samples by glow discharge plasmas at atmospheric pressure [*Laroussi et al*., 1999]. Here, the observed destruction of micron-sized Gram-negative bacteria (i.e., those possessing thin outer membranes) has been attributed to the electrostatic disruption of these membranes following their electrostatic charging [*Mendis et al*., 2000; *Laroussi et al*., 2003].

[43] In space, comets that exhibit both dust and plasma tails with significant overlap provide excellent laboratories for the study of the consequences of dust-plasma interactions, and several cometary phenomena have been explained on the basis of electrostatic disruption of dust [*Horányi and Mendis*, 1991]. Among these is an interesting class of phenomena observed in several comets, first discussed, in some detail, by *Sekanina* [1976] and subsequently by *Sekanina and Farrell* [1980], in connection with comet West 1976 V1. These are the striae or pseudosynchronic bands which are seen as relatively straight, localized, dust structures intersecting the usual synchronic dust streams (composed of dust emitted from the nucleus at a given time) at angles that make them nearly parallel to the Sun-comet radius vector. *Sekanina* [1976] pointed out that since the spatial properties of these striae do not coincide with the expected properties of truly synchronic bands that normally characterize the dust tails, they cannot be composed of grains directly ejected from the nucleus as such. While *Sekanina* [1976] argued that both gradual evaporation and sudden fragmentation of grains could be responsible for the striae, *Sekanina and Farrell* [1980] subsequently argued in favor of the latter process. They further argued that the fragmenting grains would be strongly non-spherical, being rod-like or chain-like aggregates of highly friable material. They did not however propose a physical mechanism for the fragmentation. *Hill and Mendis* [1980] proposed that the specific mechanism responsible for the disruption of the grains, was the electrostatic one discussed earlier, and that the distance down the tail, where the disruption occurred, corresponds to the distance the parent grains traveled before they acquired a charge sufficient to cause electrostatic disruption. The above authors idealized the parent grains (described as rods or chains) as prolate spheroids with a range of values for λ, the ratio of long to the short axis, and with range of values for their tensile strength, F_t. Unfortunately, by neglecting the important role of secondary electron emission in the grain-charging processes, when energetic electrons may be present (during disturbed solar wind conditions), they overestimated the surface potentials that the grains could acquire (60 V $< |\phi| <$ 300 V), which in turn led to an overestimate of the range of sizes, and the associated range of tensile strengths, of the grains that could be disrupted. While it

is unlikely that $|\phi|$ would be much larger than about 20 V even during disturbed solar wind conditions, highly friable cometary grains with $F_t < 10^5$ N/ m^2 could still be electrostatically disrupted when $|\phi| \simeq 20$ V. Thus the Rosetta mission will provide an opportunity to check the viability of the Hill-Mendis proposal for striae formation, by estimating the plasma parameters in the tail when striae are observed. Whatever the cause, it would be most useful if the process of dust disruption itself were observed in real time. Among other things, it will provide an opportunity to estimate the structural properties of cometary dust grains.

[44] Another cometary phenomenon that may be pertinent to electrostatic disruption of dust (this time on the sunward side of the nucleus) is the detection of discrete dust packets in the environment of comet Halley by the dust detectors on board Vega 1 and Vega 2 spacecraft, during their 1986 fly-bys [*Simpson et al*., 1987]. These packets of dust were detected as conspicuous events of significantly enhanced flux of fine dust with mass $m \geq 10^{-16}$ kg, lasting about 10 s each, separating regions of very low fluxes Figure 4. These authors suggested that these dust packets resulted from the break-up of larger composite grains, that left the nucleus and eventually coming unglued. *Horányi and Mendis* [1991] suggested that such a process of ungluing, presumably due to the sublimation of a volatile icy glue holding the less volatile dust grains together, would be more a gradual process than was implied by those short discrete events. They suggested, as an alternative, that such fragile composite dust aggregates could be electrostatically disrupted in the regions where they were seen; i.e., outside the ionopause where substantial electrostatic potentials of $|\phi| \approx 10 - 20$ V may be achieved. Taking the composite parent grain to be of mass $m_d \approx 10^{-15}$ kg and bulk density $\rho \approx 2 \times 10^2$ kg/m^3, leading to a radius $a \approx 1\mu$m, and for an $F_t \approx 10^3$ N/m^2, they found that electrostatic disruption would occur if $|\phi| > 16$ V. They also pointed out that if the grain is irregular, electrostatic chipping would take place even for larger values of F_t and/or smaller values of $|\phi|$. The Rosetta mission could provide an opportunity to observe such dust events together with the local plasma conditions when they occur. This could help to check if electrostatic disruption is indeed the responsible mechanism.

[45] Yet another piece of evidence for the possible occurrence of electrostatic disruption was provided by the peculiar distribution of the smallest grains, $10^{-20} < m_d < 10^{-17}$ g, also observed on the sunward side of comet Halley by the dust-impact (PUMA) mass analyzer on board Vega-1 [*Sagdeev et al*., 1989]. The most striking feature in this distribution was a sharp glitch at a cometocentric distance corresponding to the cometopause (or collisionopause) inside which the inflowing contaminated solar wind was rapidly cooled presumably by collisions with outflowing cometary neutrals [*Reme et al*., 1986]. *Formenkova and Mendis* [1992] showed that this feature in the distribution of the smallest grains could be explained by noting that cometary grains transversing the cometopause would be quickly charged from a numerically small negative potential $|\phi| \leq 1$ V, to a numerically larger one $|\phi| \approx 10$ V, when fine grains with $m \approx 10^{-16}$ g would be electrostatically disrupted, if their tensile strength $F_t \leq 5 \times 10^5$ N/m^2. This, once again, is a proposal that could either be supported or refuted by the relevant observations during the Rosetta mission.

6. SPATIAL DISTRIBUTION OF CHARGED DUST IN THE COMETARY ENVIRONMENT

[46] While the study of the dynamics of dust in the cometary environment has a long history, being initiated by the 1835 apparition of Halley's Comet [*Bessel*, 1836], the possible importance of electrostatic charging on the dynamics of the dust was recognized only much later [*Notni*, 1966]. We begin our discussion by considering the dynamics of a small, uncharged dust grain that is lifted off the cometary nucleus by the radially outflowing cometary gas. It is expected that these grains quickly reach a terminal speed v_t within the region of dust-gas interaction, which typically extends to $\approx 10R_n$ [*Mendis et al*., 1985]. Once the grain leaves this region there are only two significant forces acting on it in the heliocentric frame, the solar radiation pressure force, $F_{\rm rad}$ and the solar gravitational force, $F_{\rm grav}$, since the gravitational force of the cometary nucleus is negligible. Since both these forces vary inversely as the heliocentric distance, their ratio is a function only of the properties of the dust grains

$$\beta = \frac{F_{\rm rad}}{F_{\rm grav}} \approx \frac{6 \times 10^{-5} Q_{\rm pr}(a)}{a\rho},$$

where a and ρ are the radius and bulk density of the dust (in cgs units), respectively, and $Q_{\rm pr}(a)$ is the size-dependent scattering efficiency for radiation pressure. For dielectrics, for example Olivine, as well as conductors, for example Magnetite, $Q_{\rm pr}$ remains roughly constant in the grain size range of $2 \times 10^{-5} < a < 10^{-2}$ cm, which means that β increases inversely with grain size. When $a \leq 10^{-5}$ cm, β declines steeply, the decline being much steeper for dielectrics [*Burns et al*., 1979]. For reasonably short periods of time, $|d/\dot{d}| \ll 1$ week, (d being the comets heliocentric distance) the cometocentric frame may be regarded as an inertial one, so the only unbalanced force acting on a dust particle in this frame is the radiation pressure, directed along the Sun-comet line. This force remains approximately constant for a grain of given size, and consequently such grains emitted at various angles, with an initial speed v_i (which is the terminal speed acquired by the grain due to the drag of the outflowing gas) move in parabolic orbits, all of which are enveloped in a paraboloid of revolution (Figure 5). This is the basis of the so-called fountain model developed by *Eddington* [1910] in order to explain the pronounced near parabolic envelopes of comet Morehouse (1908c) observed in its sunward hemisphere. Eddington identified those parabolic envelopes with the projections of these bounding paraboloids on the sky. The apex distance of the paraboloid of revolution is $\alpha = v_i^2/2g_r$, where $g_r (= F_{\rm rad}/m_d)$ is the acceleration due to radiation pressure. The variation of α with grain size for Olivine and Magnetite is shown in Figure 6.

[47] Let us proceed to the consequence of grain charging on these parabolic dust orbits on the sunward side.

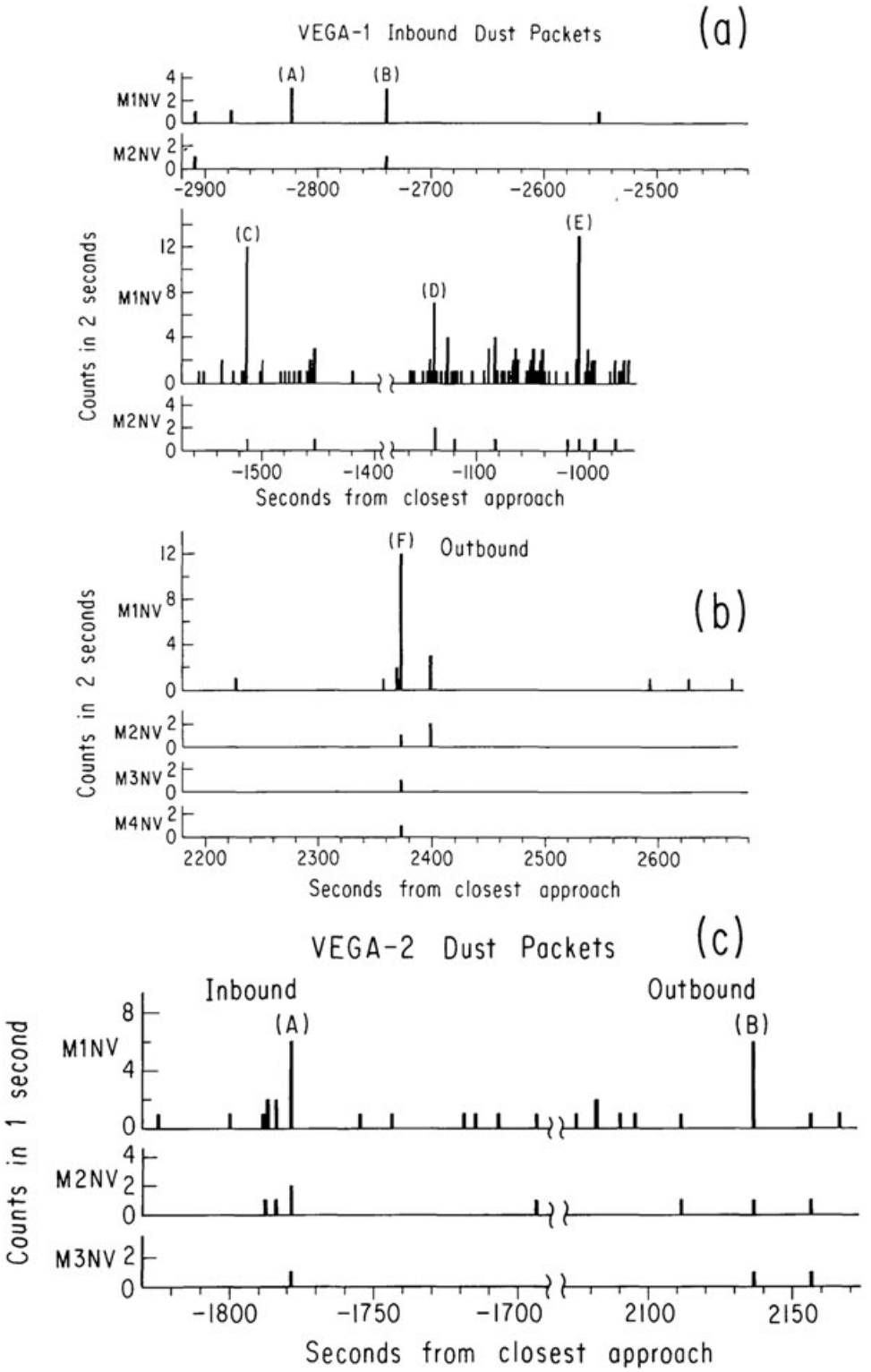

Figure 4. Time sequence of dust events observed by the DUCMA dust detector on board the (a, b) Vega 1 and (c) Vega 2 spacecraft at Halley's Comet, illustrating clusters and pockets of dust (A–F) [*Simpson et al*., 1987].

Wallis and Hassan [1983] pointed out that dust grains in the cometary environment, which are necessarily electrically charged, are subject to electrodynamic forces due to the convectional electric fields both in the undisturbed solar wind (outside the cometary bow shock) as well in the region of the shocked solar wind between this shock and the ionopause (see discussion in section 3). The electrodynamic acceleration of a grain of mass m_d, carrying a charge Q, is

$$\vec{g}_e = Q\frac{\vec{E}}{m} = -Q\frac{\vec{v}_{sw}\times\vec{B}}{m_d} \qquad (2)$$

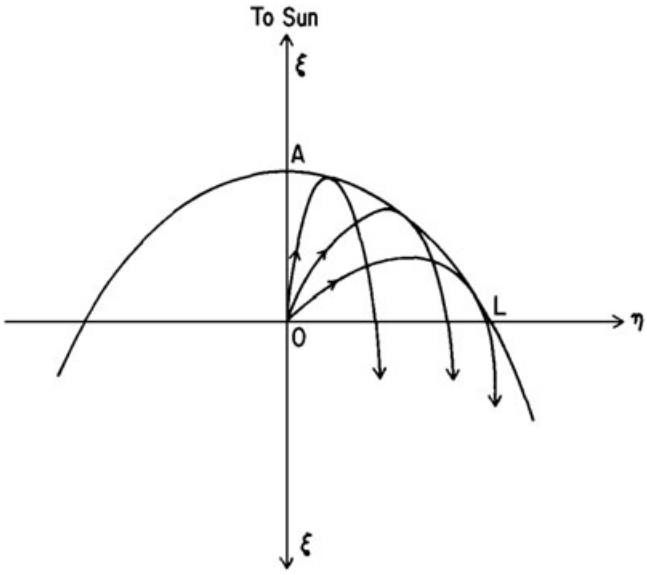

Figure 5. The parabolic trajectories and the paraboloid envelope for unchanged dust grains in a plane containing the Sun-comet axis [*Eddington*, 1910].

since $|\vec{v}_d| \ll |\vec{v}_{sw}|$ in both regions. To a good approximation $\vec{E}$ is constant outside the ionopause along the Sun-comet axis. Setting $|\vec{B}| = 5$ nT and $\vec{B}$ is inclined to $\vec{v}_{sw}$ at 45° at $d = 1$ AU, the ratio of electrostatic and gravitational accelerations becomes

$$\kappa = \frac{|g_e|}{|g_r|} = 10^{-2}\frac{|\phi(\mathrm{V})|}{Q_{pr}a(\mu)}. \quad (3)$$

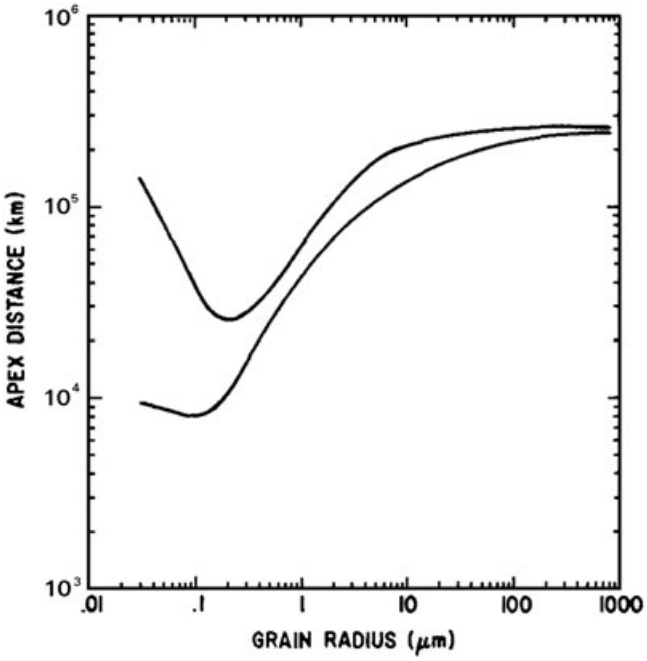

Figure 6. The apex distance of the bounding paraboloid for uncharged Olivine (upper curve) and Magnetite (lower curve) grains as a function of grain size [*Horányi and Mendis*, 1991].

TABLE 1. The Ratio of the Electric Force Over Solar Gravity, κ (From Equation (3))

a_μ	Olivine	Magnetitite
1.0	0.05	0.04
0.5	0.85	0.06
0.1	1.00	0.28
0.03	16.50	3.40

[48] The values of κ for Olivine and Magnetite are given in Table 1, taking $|\phi(\mathrm{V})| = 5$. In the cometocentric frame, these charged grains experience a total acceleration of $\vec{g}_e + \vec{g}_r$.

[49] If we provisionally assume that $\vec{g}_e$ is also constant, dust grains released isotropically, with initial speed v_i will once again follow parabolic orbits that are enveloped within a bounding parabola, oriented in the plane containing the Sun-comet axis and the convectional electric field (Figure 7). The angle, θ, measured between the direction of the axis of symmetry from the direction to the Sun, gets larger for smaller grains [*Wallis and Hassan*, 1983].

[50] If we assume that $|\phi(\mathrm{V})| = 5$ for all grains; for an olivine grain with $a = 0.1$ μm $\theta \approx 45°$, and $\theta \simeq 10°$ for a larger olivine grain with $a = 0.5$ μm.

[51] The smallest grains are inefficient scatterers of visible light and their bounding parabolas remain difficult to be remotely observed. This may not be the case for dielectric grains (e.g., Olivine) with $a \approx 0.5$ μm as their bounding parabolas have an axis inclined to the Sun-comet line at an angle that is apparent even in ground-based observations. This might have been the case in some early drawings of the sunward envelopes of comet Donati (1858v1)

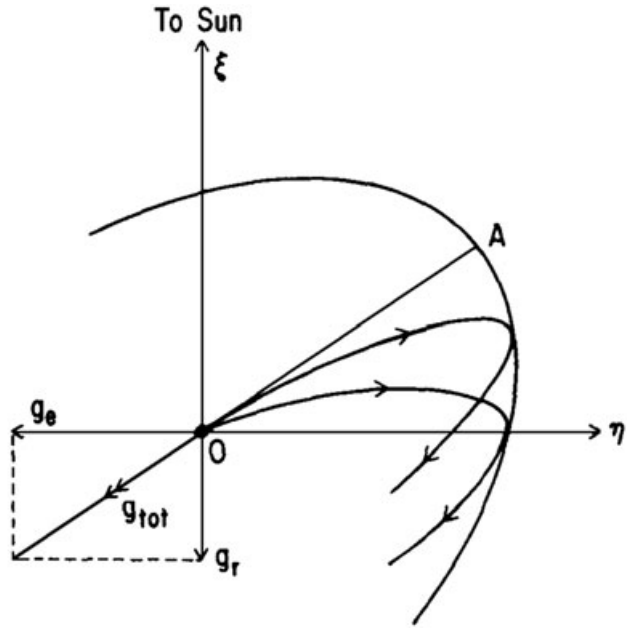

Figure 7. The parabolic trajectories and the parabola envelope of charged grains in the plane containing the Sun-comet axis and the convectional electric field vector in the cometocentric frame [*Horányi and Mendis*, 1991].

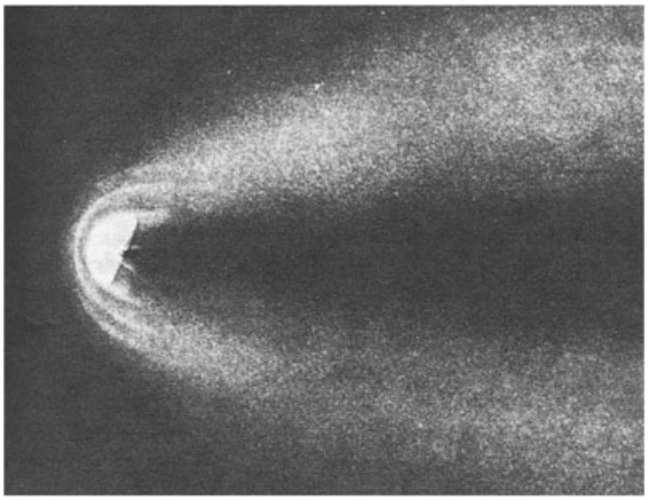

Figure 8. Drawing based on visual observations of comet Donati 1858 VI by G. P. Bond on 9 Oct 1858. The Sun comet axis is given by the prolonged tail axis [*Rahe et al*., 1969].

by the well-reputed observational astronomer, G. P. Bond (Figure 8). While it is tempting to interpret the skewness of these sunward envelopes in terms of the non-radial deceleration of fine charged (dielectric) grains, it needs to be acknowledged that an alternative explanation has been proposed by *Sekanina* [1987a, b], who interprets them in terms of spiral loci of (uncharged) grains emitted from localized regions on a rotating cometary nucleus. If the skewness of the dust distribution is due the electromagnetic forces, we expect it to vary, both periodically and intermittently, as the motion of the charged dust grains is influenced by the temporal variability of the interplanetary magnetic field. Comets high above/below the current sheet are likely to show this effect in a more pronounced way. Clearly, this is a question that could be resolved only with a detailed understanding of the dynamical properties of the cometary nucleus, the properties of the observed dust (composition, size, and charge), and the solar wind.

[52] It is important to point out that the apex distance of the bounding parabola of charged grains, is given by

$$\alpha = \frac{v_i^2}{2g_{\rm tot}} = \frac{v_i^2}{2\sqrt{g_e^2 + g_r^2}}. \qquad (4)$$

[53] While charged grains are even more compressed in the solar direction (see Figure 7) than if they were uncharged, they can move to greater distances in the direction perpendicular from the Sun-comet axis. *Horányi and Mendis* [1991] considered this as a possible explanation of the detection of very small grains by Vega 1 and Vega 2 spacecraft (inbound) at distances as large as 2.5×10^5 and 3.2×10^5 km, respectively, from the nucleus of comet Halley in 1986. These authors also pointed out that, while the precise optical properties of cometary dust grains remain unknown, even if they were absorbing (e.g., dirty silicates) as deduced from infrared thermal emissions from several comets [*Hanner*, 1980], the excursion of even the very small grains ($a = 0.05\mu$m) in the directions of the encounters were expected to be considerably less than 10^5 km.

[54] Let us now discuss the dynamics of charged dust in the cometary environment in more detail. The basic equation governing the dynamics of such a grain in the cometocentric frame, regarded as an inertial frame, is given by

$$m_d \frac{{\rm d}\vec{v}_d}{{\rm d}t} = Q(t)\left(\vec{E} + \vec{v}_d \times \vec{B}\right) + \vec{F}_{\rm rad} + \vec{F}_c + \vec{F}_{\rm ig}, \qquad (5)$$

where $\vec{E} = -\vec{v}_{\rm sw} \times \vec{B}/c$ is the convectional electric field, $\vec{F}_{\rm rad}, \vec{F}_c$, and $\vec{F}_{\rm ig}$ are the radiation pressure force, the plasma drag, and the intergrain Coulomb force, respectively. The time dependent charge $Q(t)$ can be followed using equation (1). In environments where the intergrain distance is larger than the Debye shielding distance, which is generally the case in comets, $\vec{F}_{\rm ig}$ may be neglected.

[55] In order to calculate the trajectory of charged dust particles, a model of the plasma environment is needed, including the density and temperature of the electrons and all ion species, the bulk flow field of the plasma, and the structure of the magnetic fields in the cometary environment, requiring detailed kinetic or MHD simulations.

[56] *Horányi and Mendis* [1985a] used a much simplified 'point-source-in-a-uniform-stream' model to produce the stream line structure of the plasma flow (Figure 9) and proceeded to calculate $\vec{E}(r)$, noting that the stream lines are electric equipotentials in an ideal MHD flow. While such a model is a gross oversimplification of the overall flow, it does provide a fair approximation of the streamlines obtained in more complex MHD models, and provides a useful approach to calculate the basic nature of grain trajectories.

[57] The trajectories of charged grains that remain within the region bounded by the ionopause and the outer bow

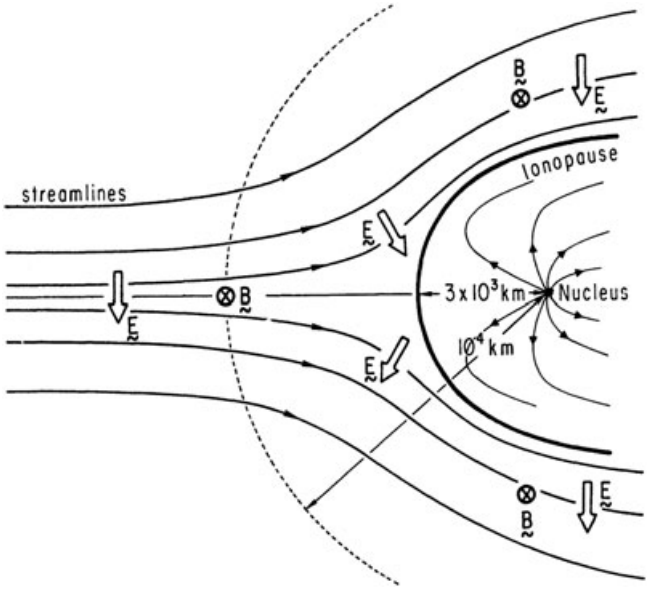

Figure 9. Schematic drawing of the plasma streamlines and the convectional electric field in the vicinity of the ionopause. The magnetic field is assumed to be into the paper [*Horányi and Mendis*, 1985b].

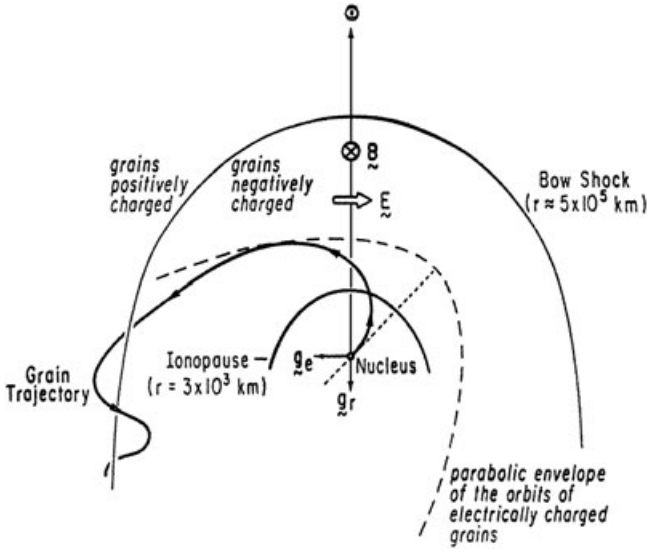

Figure 10. Schematic drawing of the trajectory of a small charged dust grain in the plane containing the Sun-comet line and the convectional electric field.

shock remains more or less parabolic, as discussed earlier. However, the trajectory of grains that penetrate the outer shock becomes more complicated because the grain charge changes sign in doing so. The trajectory of a grain penetrating the outer shock (which is estimated to occur at a speed of over 10 km/s for a particle with radius $a = 0.1$ μm) is shown in Figure 10. Due to this change of sign upon penetrating the outer bow shock, the grain may oscillate back and forth about this shock as indicated. Thus, small charged grains may be confined near the flank of this shock surface, on the side opposite to the direction of the $\vec{E}$ field. This is also a phenomenon that could be investigated during the Rosetta mission.

[58] Subsequently, [*Horányi and Mendis*, 1986a, b] performed numerical simulations of the spatial distribution of charged dust in the environments of comets Giacobini-Zinner and Halley, in anticipation of the spacecraft missions to these comets in the mid 1980s. In these simulations, they also included the effects of the orbital motion of the comet. In the case of comet Giacobini-Zinner, the spatial distribution of small grains of various sizes, in a plane normal to the Sun-comet axis at a distance of 10^4 km down the tail, is shown in Figure 11, for the case when the interplanetary magnetic field was assumed to be in the orbital plane of the comet, so that the convectional electric field is normal to this plane. Without electromagnetic effects, larger grains concentrate further away, while the smaller ones concentrate closer to the Sun-comet axis. This well-understood effect has to do with the fact that the larger grains travel for a longer time since their release from the nuclear region, than the smaller ones, due to the relatively smaller perturbation by the radiation pressure force. Electromagnetic effects can greatly distort the spatial distribution of the smallest particles, leading to their swift non-symmetrical dispersal.

[59] The NASA International Comet Explorer (ICE) spacecraft intercepted the tail of comet Giacobini-Zinner on 11 September 1985 at a distance of about 8×10^3 km tailward of the nucleus, moving generally south to north, in the comets reference frame. Although the spacecraft did not carry a dedicated dust detector, the spacecraft itself acted as a proxy, with the plasma wave instrument detecting impulsive signals that were attributed to dust impacts on the spacecraft, producing plasma clouds [*Gurnett et al*., 1986]. While a clear asymmetry in the impact rate between the inbound and outbound legs, was consistent with the predictions of *Horányi and Mendis*, [1986b], it may have been also consistent with non-isotropic emission of the grains, as suggested by *Gurnett et al*. [1986]. However, while the size of the grains could not be estimated from the signals, the larger signals were concentrated close to the axis, while the smaller ones were observed further away, exhibiting a much larger asymmetry between the inbound and outbound legs of the spacecraft trajectory. Similar observations were made by the DS1 mission at comet P/Borelly [*Tsurutani et al*., 2004].

[60] Incidentally, while the role of electrostatic charging on the dynamics of fine dust has since been established elsewhere in the solar system (e.g., planetary magnetospheres and the heliosphere [*Horányi*, 1996; *Horányi et al*., 2004], the observations at comet Giacobini-Zinner, albeit indirect and tentative, were the first spacecraft observations pertaining to charged dust in any solar system environment.

[61] The most detailed simulation of the distribution of fine charged dust in the environment of a comet was performed in connection with the spacecraft encounter of comet Halley during its 1986 apparition [*Horányi and Mendis*, 1986a]. These simulations included the orbital motion of the comet, and also the obliquity of the orbit, as well as the spin of the nucleus, as gleaned by the analysis of near-nuclear spiral features observed during its 1910 apparition [*Larson and Sekanina*, 1984; *Sekanina and Larson*, 1984]. The simulations also included both the background distribution that results from the uniform emission of dust from the sunward hemisphere and also spiral features that result from active equatorial spots on the nucleus, similar to the one inferred from the 1910 observations. As expected, the effects of charging of the grains was manifested in their distribution in the plane normal to the orbital plane, since the component of the convectional electric field is the only force in this normal plane. Since the interplanetary magnetic field switches sign with a periodicity of 5–10 days, it was anticipated that the spacecraft Vega 1 and 2, and Giotto, which followed each other 35 days apart, were likely to encounter entirely different distributions at the lower end of the dust size distribution $a \leq 0.1$ μm). The fast fly-bys of all these spacecraft were close to the orbital plane (unlike in the case of the ICE flyby of comet P/Giacobini-Zinner). As a result, the electrodynamic consequences of dust charging were missed. This however would not be the case during the extended rendezvous of the Rosetta spacecraft with comet 67P/Churyumov-Gerasimenko during 2014–2015, when it would be able to sample the evolution of the 3-D distribution of the dust in the cometary environment, over a wide range

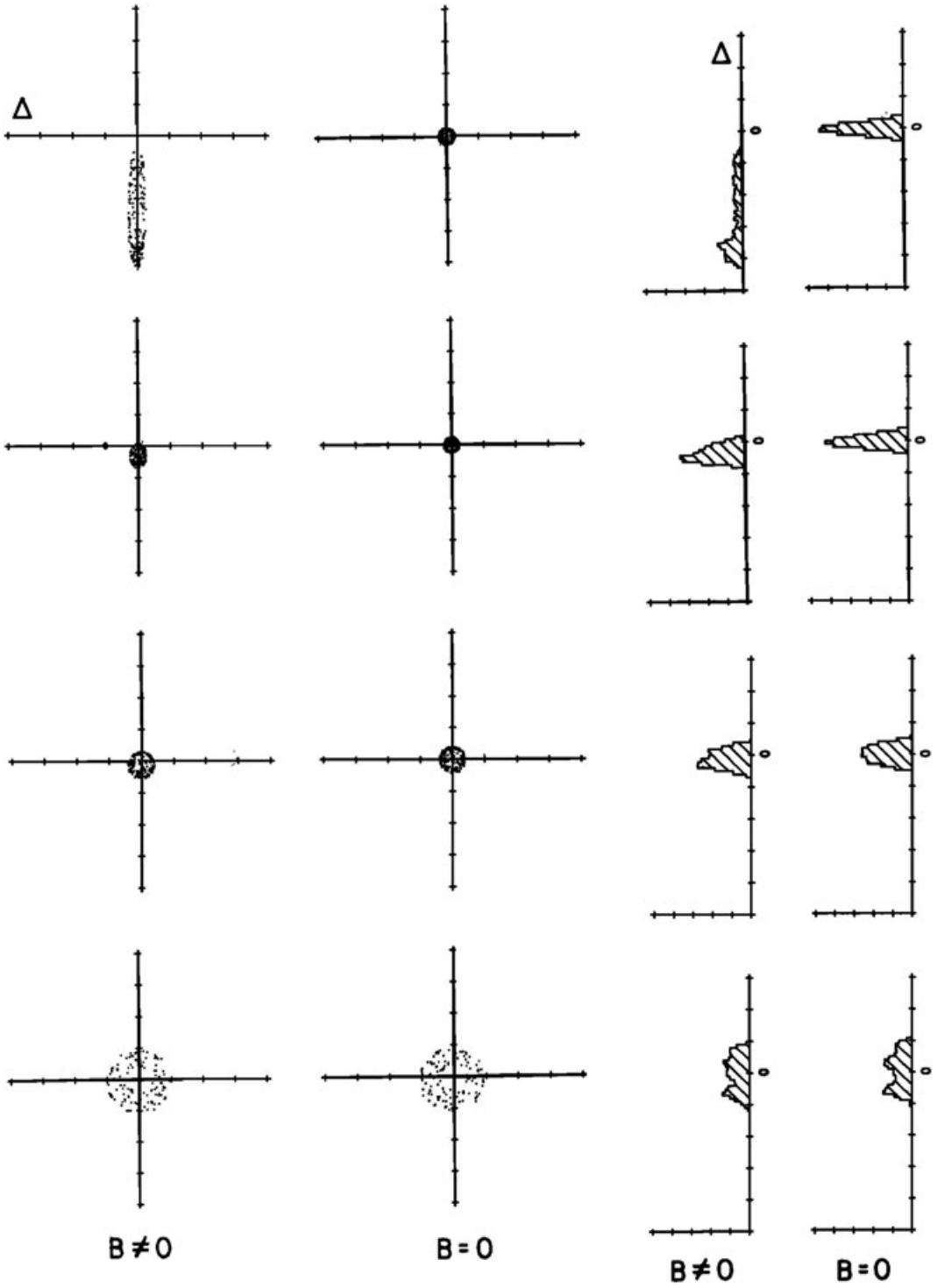

Figure 11. (Left) Two panels showing the distribution of grains with various radii (top to bottom 0.03; 0.1; 0.3; and 1 μ) in a plane normal to the Sun-comet axis at a distance of $\approx 10^4$ km behind the nucleus. The first column shows the distributions when charging effects are included ($\vec{B} \neq 0$),while the second column shows the distribution assuming the grains remain uncharged ($\vec{B} = 0$). (Right) The histograms of the column densities (in arbitrary units) corresponding to the distributions to the left. The unit length scale is $\Delta = 10^5$ km, and the nucleus is located at the origin of the coordinate system [*Horányi and Mendis*, 1986b].

of dust sizes, solar wind plasma and magnetic field conditions. We expect to acquire important information pertaining to the consequences of cometary grain charging during this mission. Also, as we acquire crucial information pertaining to the nature and morphology of the cometary nucleus and its rotational dynamics very early in the mission before strong

outgassing begins, modelers will be able to construct models of the charged dust distributions that would be encountered subsequently.

7. CROSSING A MAGNETIC SECTOR BOUNDARY: RESPONSE OF THE (CHARGED) DUST TAIL

[62] Ever since the orientation of the plasma tails of comets was used to infer the continuous outflow of plasma from the Sun, since then referred to as the solar wind [*Biermann*, 1951], comets have been used to good advantage to delineate its average global properties as well as its spatial and temporal variations. Among the many variations that are observed in the plasma tail of a comet, the most dramatic is the occasional sudden disconnection of the entire tail from the head. While this phenomenon has a long history, earlier being referred to as a "tail rejection" [*Barnard*, 1920], its systematic study began with a pioneering paper by *Niedner and Brandt* [1978], who attributed this phenomenon, which they called a "disconnection event" (DE) to the crossing of an interplanetary magnetic sector boundary, by the comet. We do not discuss the basic mechanism here except to note that it is based on magnetic field line"reconnection" at the comet's head as two adjacent regions carrying opposite magnetic polarity are pushed against each other during the passage of a magnetic sector boundary [*Mendis*, 2006; *Jia et al*., 2009; *Sekanina and Chodas*, 2012].

[63] A natural question is whether such a traversal of an interplanetary magnetic sector could produce a noticeable effect on the cometary dust tail too? This was addressed by *Horányi and Mendis* [1987]. Their basic point is that due to the reversal of the magnetic field, the convectional electric field in the flowing plasma also changes direction. This leads to the reversal of the electrodynamic acceleration of a charged dust grain as a magnetic sector boundary sweeps by it (see equation (5)). This in turn leads to a "wave-like" feature in the spatial distribution of the smaller ($a \leq 0.5\mu$m) charged dust grains, since they possess a larger charge-to-mass ratio ($\sim 1/a^2$). *Horányi and Mendis* [1987] performed numerical simulations of the evolution of the dust tail of a comet composed of fine dust grains transversing such a sector boundary (Figure 12). These authors attributed the peculiar "wavy" morphology observed down the tail of comet Ikeya-Seki (1965f) to such an effect (Figure 13).

[64] While disconnection events in the plasma tail have been observed in several comets with good correlation of magnetic sector crossings at these times [*Niedner and Brandt*, 1978], the observation of wavy features in the dust tails of comets, which *Horányi and Mendis* [1987] also attribute to the encounter of magnetic sector boundaries, is very rare. To our knowledge, the aforementioned observation of comet Ikeya-Seki is the only well-documented one in the literature. This requires an explanation, and we believe it has to do primarily with favorable geometry. Since the electrodynamic consequences of such an encounter are most apparent normal to the orbital plane of the comet, they could be best observed when the magnetic field vector of the solar wind encountering the comet lies in a plane close to the orbital plane of the comet. Also, the optimal observing geometry would allow for imaging the dust tail in forward-scattered light. Reversals of the interplanetary magnetic field occur with a quasi periodicity of 5–10 days. The Rosetta spacecraft moving with the comet for over a year is expected to witness the emergence of a significant dust tail. The spacecraft will observe the three-dimensional global distribution of the dust, including the grains ($a \leq 0.5$ μm) at relatively close range, as well as taking images at a variety of phase-angles of the large-scale dust environment. We therefore expect that it may detect the change in the spatial distribution of the charged dust during the passage of a magnetic sector boundary across the tail, leading to the wavy dust structures.

8. WAVES IN DUSTY PLASMAS: POSSIBLE ROLE IN COMETS

[65] The presence of charged dust can alter collective behavior of the plasma as manifested by altered dispersion relationships of the customary plasma waves, and the emergence of new plasma waves and instabilities [*Verheest*, 2000; *Shukla and Mamun*, 2002; *Bliokh et al*., 1995; *Tsytovich et al*., 2008] In the following, we describe dusty plasma wave modes and an instability that possibly have relevance to comets.

[66] First, we discuss the so-called "Dust Ion Acoustic" (DIA) mode predicted by *Shukla and Silin* [1992] and first observed in the laboratory [*Barkan et al*., 1996]. Here, the charged dust does not participate in the wave dynamics; it simply modifies the wave mode via the quasi-neutrality condition in the plasma. If we consider the simple case of dust particles (all of the same size) in a singly ionized two-component (electron and ion) thermal plasma, where the only charging currents to the grains are electron and ion collection, the grains become negatively charged (as discussed in section 2). If each dust grain carries an excess of Z electrons on its surface, the quasi-neutrality condition in the undisturbed plasma is as follows:

$$n_{i0} = n_{e0} + Zn_{d0}, \tag{6}$$

where $n_{\alpha 0}$ refers to the ion, electron, and dust number densities in the undisturbed plasma. Note that this leads to a depletion in the electron density relative to the ion density. This increases the phase velocity of a DIA wave above the usual ion acoustic wave in a dust-free plasma. With the approximation of negligible electron inertia and immobile dust grains, the dispersion relation for the DIA wave is given by *Shukla and Silin* [1992]

$$\omega^2 = \frac{\delta k^2 c_s^2}{1 + k^2 \lambda_{\mathrm{De}}^2}, \tag{7}$$

where $c_s = (k_B T_e/m_i)^{1/2}$ is the usual ion acoustic speed, λ_{De} is electron Debye shielding length, and $\delta = (n_{i0}/n_{e0})$. In the long-wavelength regime ($k\lambda_{\mathrm{De}} \ll 1$), equation (7) reduces to

$$\omega = k\delta^{1/2} c_s. \tag{8}$$

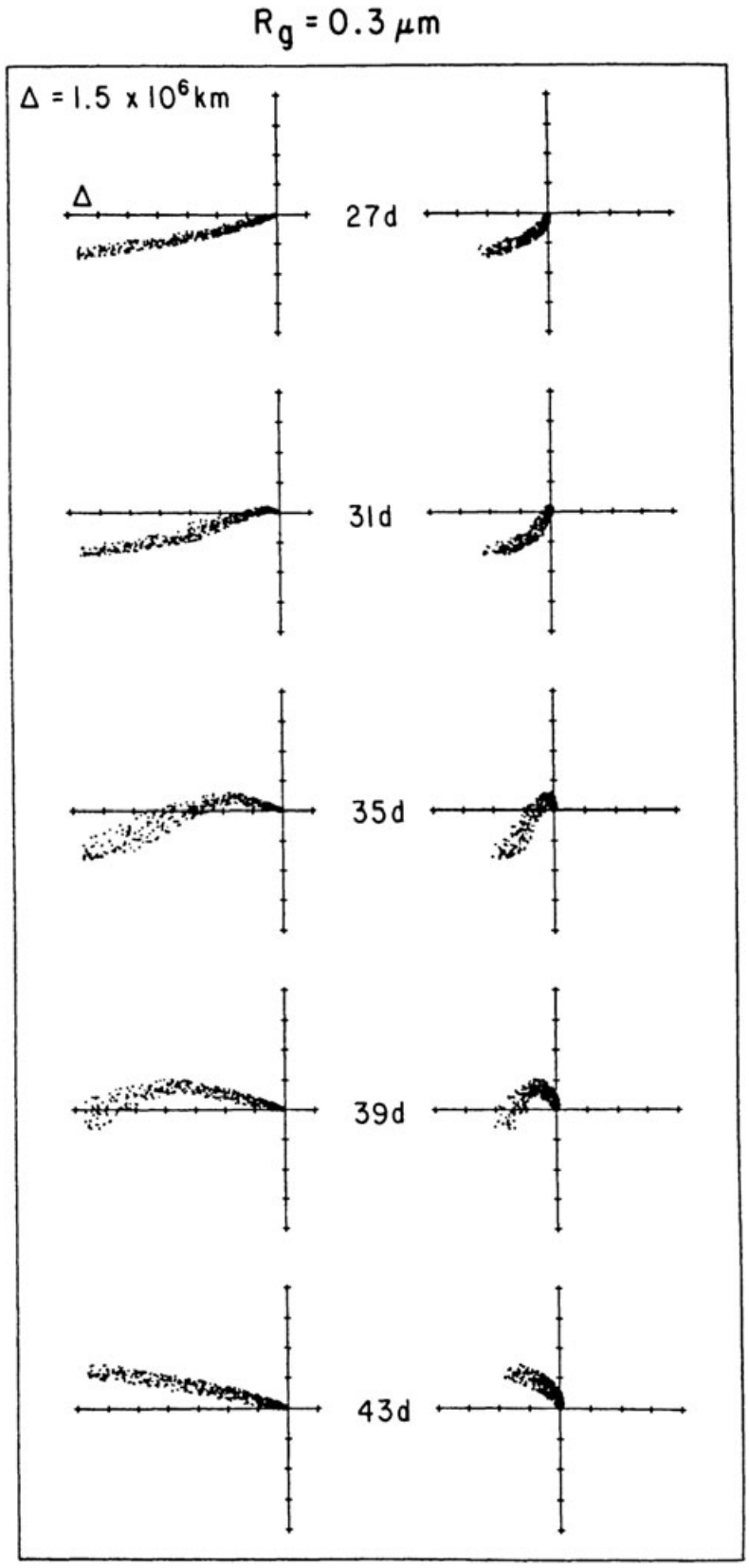

Figure 12. Time evolution of the charged dust tail of a comet on crossing a magnetic sector boundary. All grains are assumed to be of equal radius (a = 0.3 μm). The left panels show the projections of the evolution of the dust distributions 2 days apart, in a plane normal to the orbital plane of the comet and containing the sun-comet axis. The sun is to the right and the sense of orbital motion is into the paper. The panels on the right show the corresponding projections in a plane normal to the sun-comet axis. Here, the motion is to the right [*Horányi and Mendis*, 1987].

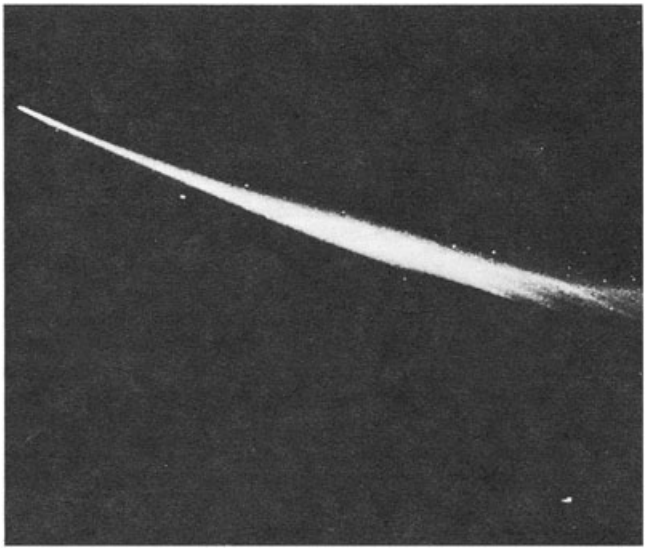

Figure 13. The dust tail of comet Ikeya-Seki, (1965f). Note the well-defined wavy structure far down the tail (Kodaikanal Observatory photograph).

[67] Since $\delta^{1/2}$ could be $\gg 1$ if the electron depletion due to dust is sufficiently large, the phase velocity (ω/k) of this wave could be $\gg c_s$. Consequently, its Landau damping could be negligible even in the case of an isothermal ($T_e = T_i$) plasma. This is in contrast to a pure electron-ion plasma, where $T_e \gg T_i$ is required for the acoustic wave to be undamped. The implication of this in various cosmic dusty plasma environments was discussed by *Mendis and Rosenberg* [1994]. In particular, they considered the existence of the "inner" shock just inside the cometary ionopause (see section 1). While observations of the ion density and flow profiles [*Goldstein et al*., 1989; *Schwenn et al*., 1987] just inside the ionopause during the Giotto mission to comet Halley was shown to be consistent with the existence of such a shock [*Damas and Mendis*, 1992], its nature remains unclear. It was expected that its formation was mediated by the ion acoustic wave, which required that $T_e \gg T_i$. While a detailed, multi-fluid model of the cometary ionosphere [*Marconi and Mendis*, 1983] indicated that $T_e \simeq 3T_i$ close to the ionopause, where this shock was expected to form. It is not clear if this temperature disparity is sufficient to suppress the Landau damping of the ion acoustic wave. Consequently, *Mendis and Rosenberg* [1994] suggested that the existence of charged dust in this region could give rise to the DIA, which would be undamped, and thus could be what mediates this cometary inner shock. This however would require that the dust inter-grain distance d_d, is sufficiently smaller than Λ_D. Whether this is the case is also not clear. In fact, the estimates of $d_d/\Lambda_d \simeq 1$ inside the ionopause, whereas it is ≥ 10 outside the ionopause, where the convectional electric field operates [*Mendis*, 2002]. So the nature of the wave that mediates the inner shock is an open question. Perhaps both processes (i.e., temperature disparity and the role of dust) operate in concert. It also needs to be pointed out that using a 1-D flow model that reproduced the electron heating in the outer cometary ionosphere [*Marconi and Mendis*, 1983, *Körösmezey et al*. [1987] argued for the existence of an inner shock of an electrostatic nature, without the need for charged dust. The observations of the outer regions of the cometary ionosphere during the Rosetta mission will help to resolve this question.

[68] Several authors have considered the excitation of the dust ion acoustic instability in the Saturnian magnetosphere, due to the relative motion of the co-rotating plasma and the charged dust particles moving with speeds intermediate between co-rotation and the local Kepler velocity [*Rosenberg*, 1993; *Winske et al*., 1995]. Both the linear and the non-linear properties of this instability have been investigated, including its saturation due to the trapping of plasma ions. It has been identified as a possible explanation for the temperature increase of O^+ ions in the region 4–8 R_S from about 40–200 eV, first observed by the Voyager mission at Saturn [*Richardson and Sittler*, 1990]. There is also relative motion between the charged dust and the plasma throughout the cometary dusty plasma environment, in both the cometary head and the tail. Perhaps, a good candidate location is the region behind the nucleus where the already high speed ions forming the ion-tail diverge from the flow of dust into the dust tail of 67P/Churyumov-Gerasimenko.

[69] The second dusty plasma wave mode to consider is the so-called "Dust Acoustic" (DA) mode, whose existence was predicted by *Rao et al*. [1990], and spectacularly observed in the laboratory by *Barkan et al*. [1995]. In this case, contrary to the DIA mode, the charged dust grains also participate in the wave dynamics, in addition to modifying the usual quasi-neutrality condition. The laboratory experiment, shown in Figure 14, used a potassium plasma with $k_B T_e \simeq 3$ eV, $k_B T_i \simeq 0.2$ eV, micron sized dust grains of equal mass $m \simeq 10^{-15}$ kg, a typical dust charge of $Z_d \simeq 2 \times 10^3$e, and had $n_d/n_i \simeq 5 \times 10^{-4}$. In this setup, a slowly propagating ($v_\varphi \simeq 9$ cm/s), long wavelength ($\lambda \simeq 0.6$ cm), low frequency ($\omega \simeq 15$ Hz), longitudinal wave of significant amplitude ($A = |\Delta n_d/n_{d0}| \simeq 1$) was observed by laser scattering. With these conditions (i.e., $k_B T_e \gg kT_i$), in the long-wavelength regime ($k\lambda_{\mathrm{De}} << 1$) the dispersion relation of the DA mode reduces to [*Rao et al*., 1990]

$$\omega^2 = Z_d^2 k^2 \left(\frac{k_B T_i}{m_d} \frac{n_{d0}}{n_{i0}} \right). \tag{9}$$

Substituting the experimental values in equation (9) results $v_\varphi = \omega/k \simeq 10$ cm/s, in a good agreement with the observed value.

[70] The possibility of observing such waves in the dusty plasma environment of comets has not been discussed in the literature, and owing to their small spatial scales, could not have been possibly observed during the fly-by missions to date. The high-resolution cameras onboard Rosetta might be able to capture the propagating small-scale structures of possible DA waves. Perhaps, new dusty plasma phenomena will be found by Rosetta that could lead to the inference of the excitation of DIA and DA waves and instabilities.

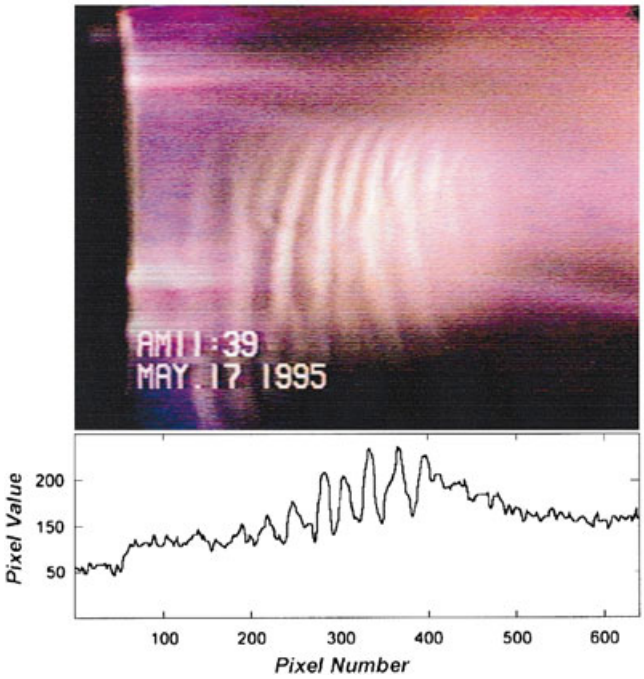

Figure 14. Single video frame image of a Dust Acoustic Wave (DAW). The bright vertical bands correspond to the wave crests (dust compressions). The bluish-red glow is the light emission from the plasma. The entire image covers 640 (vertical) pixels by 320 (horizontal) pixels. The bottom plot is the horizontal intensity map (pixel values) of pixel row 200. The wavelength of this DAW $\lambda \simeq 0.6$ cm was measured directly from a single frame video image. The wave phase velocity $v_\varphi \simeq 9$ cm/s was determined from an analysis of successive frames of video images [*Thompson et al*., 1999].

[71] The two-stream plasma instability associated with the counter streaming of charged dust has been discussed by *Havnes* [1980], concluding that the conditions for its onset are unlikely to be met anywhere in our solar system. A more likely scenario for the excitation of this type of an instability is due to the relative motion of charged dust and the plasma in cometary tails is the DIA instability. Large-scale wave phenomena observed down the plasma tail of several comets have been attributed to the Kelvin-Helmholtz instability, excited by the velocity shear between the solar wind and cometary plasma flows [*Ershkovich*, 1980]. Perhaps this question too needs to be revisited to include the effects of charged dust in this environment.

9. THE ROSETTA MISSION

[72] Rosetta is the first mission capable of long-term monitoring of a comet. It was launched in March 2004 to study the origin of comets, the relationship between cometary and interstellar material, and its implications about the origin and evolution of our solar system. Rosetta performed three gravity assists at the Earth and one at Mars in order to reach 67P/Churyumov-Gerasimenko [*Glassmeier et al*., 2007; *Schulz*, 2009]. Rosetta performed close fly-bys of asteroids (2867) Steins and (21) Lutetia, in 2008 and 2010, respectively, and collected remarkable observations of these objects [*Accomazzo et al*., 2010; *Schulz*, 2009; *Schulz et al*., 2012].

[73] Rosetta will rendezvous with comet 67P/Churyumov-Gerasimenko in May 2014 at about 4 AU away from the Sun, and enter a close orbit in August 2014 at a heliocentric distance of $d = 3.6$ AU. The orbiter carries 11 instruments to continually observe the nucleus and the coma through a variety of remote sensing instruments, as well as the plasma, neutral gas and dust environment via in situ measurements [*Glassmeier et al*., 2007; *Schulz*, 2009]. The spacecraft will fly as low as a few kilometers from the surface to obtain high-resolution images of the nucleus. In November 2014 Rosetta will deliver a small lander Philae, with 9 instrument packages to the surface of the comet. At this time 67P/Churyumov-Gerasimenko will be at a heliocentric distance of $d = 3.0$ AU and is expected to be still in a low state of activity. Philae, named after the island in the Nile, where the obelisk was found that was used, together with the Rosetta Stone, to decipher Egyptian hieroglyphs. Philae is designed to touch down on the nucleus, deploying harpoons to anchor itself to its surface, and it is expected to survive and continue to make measurements for several days [*Glassmeier et al*., 2007; *Schulz*, 2009].

[74] Rosetta will bring closure to many open questions about comets, and their possible role in the emergence of life on Earth. In addition to many contributions to our understanding of the formation and evolution of our solar system, Rosetta will also provide an excellent opportunity to learn about the basic physics of dusty plasmas in a cometary environment.

[75] The Rosetta mission carries perhaps the most comprehensive set of instruments of any space mission to date [*Glassmeier et al*., 2007]. Table 2 lists all the instruments and their scientific objectives onboard the orbiter and the lander.

[76] Dust particles on the surface of the comet or in the coma of 67P/Churyumov-Gerasimenko adjust their electrostatic charges as dictated by the changing plasma conditions, and they act as active electrostatic probes, continuously adjusting their surface potential towards the local equilibrium value. The fields and particles environment of the comet can uniquely shape the size and the spatial distribution of the dust grains, connecting the observations of a surprisingly large number of the Rosetta instruments.

[77] 1. Dust detectors (COSIMA, GIADA, MIDAS, SESAME-DIM) provide in situ measurement of the mass and the velocity of the dust grains.

[78] 2. Plasma detectors (ROSINA, RPC-IES, RPC-ICA, ROMAP-SPM) provide the composition,density, and energy distribution of the plasma. The data can be used to calculate the charging currents of the grains, and to learn whether grains are in charge equilibrium or will have significant charge variations due to fluctuations and/or gradients in composition and/or density and/or temperature of the plasma.

TABLE 2. Instruments Onboard the Rosetta Orbiter and the Philae Lander [*Glassmeier et al.*, 2007]

Instrument	Scientific Objective
ORBITER	
ALICE	UV-Spectrometer
CONSERT	Radio Sounding and Nucleus Topography
COSIMA	Dust Mass Spectrometer
GIADA	Dust Velocity and Impact Momentum
MIDAS	Grain Morphology with an Atomic Force Microscope
MIRO	Microwave Spectroscopy
OSIRIS	Color Imaging with Narrow And Wide Angle Cameras
ROSINA	Neutral Gas and Ion Spectroscopy
RPC-ICA	Ion Composition Analyzer
RPC-IES	Ion and Electron Sensor
RPC-LAP	Langmuir Probe
RPC-MAG	Magnetometer
RPC-MIP	Mutual Impedance Probe
RSI	Radio Science
SREM	Radiation Environment Monitor
VIRTIS	VIS and IR Mapping Spectroscopy
LANDER	
APXS	α-p-X-Ray Spectrometer
CIVA	Panoramic Camera and IR Microscope
CONSERT	Nucleus Sounding
COSAC	Elemental and Composition Gas Analyzer
MUPUS	Surface and Subsurface Science
PTOLEMY	Isotopic Composition
ROLIS	Descent Camera
ROMAP-ROMAG	Magnetometer
ROMAP-SPM	Plasma Monitor
SD-2	Drill and Sample
SESAME-DIM	Dust Impact Monitor
SESAME-CASSE	Acoustic Surface Sounding
SESAME-PP	Permittivity Probe

[79] 3. Magnetometers (RPC-MAG, OMAP-ROMAG) provide magnetic field measurements. The data are essential to calculate the trajectories of charged dust particles, and the large-scale structure of the dust density distribution.

[80] 4. Imaging experiments (OSIRIS, VIRTIS, CIVA, ROLIS) supply images at various wavelength and phase angles to show the spatial and size distribution of the dust particles. Ultimately, the spatial distributions of the fine dust can be independently modeled based on the transport processes identified to be at work from in situ experiments, and compared with the images.

[81] It will be a unique and powerful consistency test if our models describing dust transport, based on particles and fields data, match the observations of the dust detectors and the images.

10. SUMMARY AND OUTLOOK

[82] Comets provide excellent laboratories to study dusty plasma phenomena in space. Perhaps most remarkable is the fact that these laboratories are not static. As a comet approaches the Sun from a large distance, its particles and fields environment changes dramatically (section 3). This leads to a wide range of dust-plasma interactions with both physical and dynamical consequences for the dust (sections 4–7), as well as the dusty plasma ensemble as a whole via possible collective effects (section 8).

[83] Dusty plasma phenomena have been observed at a wide range of cometary activities, beginning with an inactive distant comet where the solar wind flows unimpeded on to the surface, to comets closer to perihelion, when the solar wind interacts with an extended, dense commentary atmosphere. However, all of the existing observations pertain to different comets at different heliocentric distances. Also, the methods have ranged from ground-based and Earth-orbiting observations, to in situ measurements from fast fly-by spacecraft (section 1).

[84] Unlike the observations to date, Rosetta will rendezvous with comet 67P/Churyumov-Gerasimenko in May 2014, at about 4 AU from the Sun, deploy its Philae surface lander in November 2014, and escort the comet around the Sun until at least December 2015 (section 9). Consequently, due to its impressively complete set of instruments to observe the nucleus, the evolving fields and particles, and dust environment of the comet, we expect to gain an unprecedented insight into a range of interconnected dusty plasma phenomena, observed so far only in fragments, at different comets at different heliocentric distances. Initially, we expect to learn about surface interactions, the charging, mobilization, and transport of dust on the nucleus. These processes have relevance to all airless bodies in the solar system, including Mercury, the Moon, asteroids, and the martian moons Phobos and Deimos, for example. Rosetta will follow the emergence of the cometary atmosphere and ionosphere, the dramatically changing interaction of the comet with the solar wind plasma flow, and its effects on the size and spatial distributions of dust.

[85] The multi-spacecraft observations of comet 76P/Halley during its last apparition in 1986 greatly enhanced

our knowledge about comets, and gave rise to the recognition of the important role dusty plasma processes can play at comets. It is our expectation that the Rosetta/Philae rendezvous mission to comet 67P/Churyumov-Gerasimenko would bring closure to many open questions about comets, and the physics of dusty plasmas in cometary environments, while possibly observing a range of as of yet unseen and unpredicted phenomena.

[86] **Acknowledgments.** D.A.M. acknowledges support from US DOE grant DF-FG02-04ER54852. M.H. was supported by the NASA Lunar Science Institute's Colorado Center for Lunar Dust and Atmospheric Studies.

[87] The Editor of this paper was Mark Moldwin. He thanks two anonymous reviewers for their review assistance on this manuscript.

[88] During the writing of this review, we received the sad news of the death of our dear friend and esteemed colleague, Prof. Padma K. Shukla (1950–2013). Prof. Shukla pioneered the study of collective processes in dusty plasmas. He set the highest standards in his prolific scientific research and in his generous collaboration with young researchers throughout the world. He will be sorely missed. The present review is dedicated to his memory.

REFERENCES

Accomazzo, A., K. R. Wirth, S. Lodiot, M. Küppers, and G. Schwehm (2010), The flyby of Rosetta at asteroid Steins—Mission and science operations, *Planet. Space Sci.*, *58* (9), 1058–1065, doi:10.1016/j.pss.2010.02.004.

A'Hearn, M. F., et al. (2005), Deep impact: Excavating comet Tempel 1, *Science*, *310*, 258–264, doi:10.1126/science.1118923.

Barkan, A., R. L. Merlino, and N. D'Angelo (1995), Laboratory observation of the dust-acoustic wave mode, *Phys. Plasmas*, *2*, 3563–3565, doi:10.1063/1.871121.

Barkan, A., N. D'Angelo, and R. L. Merlino (1996), Experiments on ion-acoustic waves in dusty plasmas, *Planet. Space Sci.*, *44*, 239–242, doi:10.1016/0032-0633(95)00109-3.

Barnard, E. E. (1920), On Comet 1919b and on the rejection of a comet's tail, *Astrophys. J.*, *51*, 102, doi:10.1086/142527.

Bessel, F. W. (1836), Beobachtungen uber die physische Beschaffenheit des Halley's schen Kometen und dadurch veranlasste Bemerkungen, *Astron. Nachr.*, *13*, 185–232.

Biermann, L. (1951), Kometenschweife und solare Korpuskularstrahlung, *Z. Astrophys.*, *29*, 274.

Bliokh, P., V. Sinitsin, and V. Yaroshenko (1995), *Dusty and Self-Gravitational Plasmas in Space*, 268 pp., Kluwer Academic Publishers (Astrophysics and Space Science Library), Dordrecht, Boston.

Bouchoule, A., and L. Boufendi (1993), Particulate formation and dusty plasma behaviour in argon-silane RF discharge, *Plasma Sources Sci. Technol.*, *2*, 204–213, doi:10.1088/0963-0252/2/3/011.

Brandt, J. C (1987), The nature of comets, *R. Soc. London, Ser. A*, *323*, 437–445, doi:10.1098/rsta.1987.0097.

Brandt, J. C. (1990), *Comet Halley: Investigations, Results, Interpretations*, pp. 33–55, The large-scale plasma structure of Halley's comet, 1985 - 1986, Ellis Horwood, NY.

Brownlee, D., et al. (2006), Comet 81P/Wild 2 under a microscope, *Science*, *314*, 1711, doi:10.1126/science.1135840.

Burns, J. A., P. L. Lamy, and S. Soter (1979), Radiation forces on small particles in the solar system, *Icarus*, *40*, 1–48, doi:10.1016/0019-1035(79)90050-2.

Chow, V. W., D. A. Mendis, and M. Rosenberg (1993), Role of grain size and particle velocity distribution in secondary electron emission in space plasmas, *J. Geophys. Res.*, *98*(19), 065, doi:10.1029/93JA02014.

Coates, A., and G. Jones (2009), Plasma environment of Jupiter family comets, *Planet. Space Sci.*, *57* (10), 1175–1191, doi:10.1016/j.pss.2009.04.009.

Combi, M. R., V. M. Tenishev, M. Rubin, N. Fougere, and T. I. Gombosi (2012a), Narrow dust jets in a diffuse gas coma: A natural product of small active regions on comets, *Astrophys. J.*, *749*, 29, doi:10.1088/0004-637X/749/1/29.

Combi, M. R., V. M. Tenishev, M. Rubin, N. Fougere, and T. I. Gombosi (2012b), Erratum: "Narrow dust jets in a diffuse gas coma: A natural product of small active regions on comets" (2012, ApJ, 749, 29), *Astrophys J.*, *758*, 144, doi:10.1088/0004-637X/758/2/144.

Criswell, D. R., and B. R. De (1977), Intense localized photoelectric charging in the lunar sunset terminator region. I - Development of potentials and fields. II - Supercharging at the progression of sunset, *J. Geophys. Res.*, *82*, 999–1007.

Cui, C., and J. Goree (1994), Fluctuations of the charge on a dust grain in a plasma, *IEEE Trans. Plasma Sci.*, *22*, 151–158, doi:10.1109/27.279018.

Damas, M. C., and D. A. Mendis (1992), A three-dimensional axisymmetric photochemical flow model of the cometary 'inner' shock layer, *Astrophys. J.*, *396*, 704–710, doi:10.1086/171752.

Davis, V. A., M. J. Mandell, and M. F. Thomsen (2008), Representation of the measured geosynchronous plasma environment in spacecraft charging calculations, *J. Geophys. Res. A: Space Phys.*, *113*, A10204, doi:10.1029/2008JA013116.

de Almeida, A. A., D. Trevisan Sanzovo, G. C. Sanzovo, R. Boczko, and R. Miguel Torres (2009), *Adv. Space Res.*, *43*, 1993–2000, doi:10.1016/j.asr.2009.01.031.

Eddington, A. S. (1910), The envelopes of comet Morehouse (1908c), *Monthly Notices of the RAS*, *70*, 442–458.

Ershkovich, A. I. (1980), Kelvin-Helmholtz instability in type-1 comet tails and associated phenomena, *Space Sic. Rev.*, *25*, 3–34, doi:10.1007/BF00200796.

Flammer, K., T. E. Birmingham, D. A. Mendis, and T. G. Northrop (1992), A self-consistent model for the particles and fields upstream of an outgassing comet. II - A time-dependent description, *J. Geophys. Res.*, *97*, 8173–8181, doi:10.1029/92JA00145.

Flammer, K. R. (1988), The variable nature of the comet-solar wind interaction, Ph.D. thesis, California Univ., San Diego.

Flammer, K. R. (1991), The global interaction of comets with the solar wind, in *IAU Colloq. 116: Comets in the post-Halley era, astrophysics and space science library*, edited by R. L. Newburn, J., M. Neugebauer, and J. Rahe, vol. 167, pp. 1125–1144.

Flammer, K. R., and D. A. Mendis (1991), A note on the mass-loaded MHD flow of the solar wind towards a cometary nucleus, *Astrophys. Space Sci.*, *182*, 155–162, doi:10.1007/BF00646450.

Flammer, K. R., and D. A. Mendis (1993), The flow of the contaminated solar wind at comet P/Grigg-Skjellerup, *J. Geophys. Res.*, *98*, 21,003, doi:10.1029/93JA02530.

Flammer, K. R., B. Jackson, and D. A. Mendis (1986), On the brightness variations of Comet Halley at large heliocentric distances, *Earth Moon Planets*, *35*, 203–212, doi:10.1007/BF00058065.

Flammer, K. R., D. A. Mendis, V. D. Shapiro, and V. I. Shevchenko (1993), The solar wind interaction with Comet P/Grigg-Skjellerup, *Earth Moon Planets*, *60*, 31–40, doi:10.1007/BF00612178.

Flanagan, T. M., and J. Goree (2006), *Phys. Plasmas*, *13* (12), 123,504, doi:10.1063/1.2401155.

Formenkova, M. N., and D. A. Mendis (1992), Note on the very small grains (VSGs) observed at halley's comet, *Astrophys. Space Sci.*, *189*, 327–331.

Galeev, A. A. (1987), Encounters with comets—Discoveries and puzzles in cometary plasma physics, *Astron. Astrophy*, *187*, 12

Glassmeier, K.-H., H. Boehnhardt, D. Koschny, E. Kührt, and I. Richter (2007), The Rosetta mission: Flying towards the origin of the solar system, *Space Sic. Rev.*, *128*, 1–21, doi:10.1007/s11214-006-9140-8.

Goertz, C. K. (1989), Dusty plasmas in the solar system, *Rev. Geophys.*, *27*, 271–292, doi:10.1029/RG027i002p00271.

Goertz, C. K., and W.-H. Ip (1984), Limitation of electrostatic charging of dust particles in a plasma, *Geophys. Res. Lett.*, *11*, 349–352, doi:10.1029/GL011i004p00349.

Goldstein, B. E., K. Altwegg, H. Balsiger, S. A. Fuselier, and W.-H. Ip (1989), Observations of a shock and a recombination layer at the contact surface of Comet Halley, *J. Geophys. Res.*, *94*, 17,251–17,257, doi:10.1029/JA094iA12p17251.

Gurnett, D. A., T. F. Averkamp, F. L. Scarf, and E. Grun (1986), Dust particles detected near Giacobini-Zinner by the ICE plasma wave instrument, *Geophys. Res. Lett.*, *13*, 291–294, doi: 10.1029/GL013i003p00291.

Hanner, M. S. (1980), Physical characteristics of cometary dust from optical studies, in *Solid Particles in the Solar System, IAU Symposium*, edited by I. Halliday, and B. A. McIntosh, vol. 90, D. Reidel Pub.Co, Dordrecht-Holland, pp. 223–235.

Hartogh, P., et al. (2011), Ocean-like water in the Jupiter-family comet 103P/Hartley 2, *Nature*, *478*, 218–220, doi: 10.1038/nature10519.

Havnes, O. (1980), A two-stream instability in streams of charged grains, in *Solid particles in the solar system, IAU symposium*, edited by I. Halliday, and B. A. McIntosh, vol. 90, D. Reidel Pub.Co, Dordrecht-Holland, pp. 315–318.

Havnes, O., C. K. Goertz, G. E. Morfill, E. Gruen, and W. Ip (1987), Dust charges, cloud potential, and instabilities in a dust cloud embedded in a plasma, *J. Geophys. Res.*, *92*, 2281–2287, doi: 10.1029/JA092iA03p02281.

Hill, J. R., and D. A. Mendis (1980), On the origin of striae in cometary dust tails, *Astrophys. J.*, *242*, 395–401, doi: 10.1086/158472.

Hill, J. R., and D. A. Mendis (1981), Electrostatic disruption of a charged conducting spheroid, *Can. J. Phys.*, *59*, 897–901, doi: 10.1139/p81-116.

Horányi, M. (1996), Charged dust dynamics in the solar system, *Annu. Rev. Astron Astr.*, *34*, 383–418., doi:10.1146/annurev.astro.34.1.383.

Horányi, M., and C. K. Goertz (1990), Coagulation of dust particles in a plasma, *Astrophys. J.*, *361*, 155–161, doi:10.1086/169178.

Horányi, M., and D. A. Mendis (1985a), Trajectories of charged dust grains in the cometary environment, *A. J.*, *294*, 357–368, doi:10.1086/163303.

Horányi, M., and D. A. Mendis (1985b), Trajectories of charged dust grains in the cometary environment, *Astrophys. J.*, *294*, 357–368, doi:10.1086/163303.

Horányi, M., and D. A. Mendis (1986a), The effects of electrostatic charging on the dust distribution at Halley's Comet, *Astrophys. J.*, *307*, 800–807, doi:10.1086/164466.

Horányi, M., and D. A. Mendis (1986b), The dynamics of charged dust in the tail of Comet Giacobini-Zinner, *J. Geophys. Res.*, *91*, 355–361, doi:10.1029/JA091iA01p00355.

Horányi, M., and D. A. Mendis (1987), The effect of a sector boundary crossing on the cometary dust tail, *Earth Moon Planets*, *37*, 71–77, doi:10.1007/BF00054325.

Horányi, M., and D. A. Mendis (1991), The electrodynamics of charged dust grains in the cometary environment. Comets in the Post-Halley Era (eds.: R.L. Newburn, M. Neugebauer and J. Rahe), *2*, 1093–1104

Horányi, M., T. W. Hartquist, O. Havnes, D. A. Mendis, and G. E. Morfill (2004), Dusty plasma effects in Saturn's magnetosphere, *Rev. Geophys.*, *42*, RG4002, doi:10.1029/2004RG000151.

Intriligator, D. S., and M. Dryer (1991), A kick from the solar wind as the cause of Comet Halley's February 1991 flare, *Nature*, *353*, 407–409, doi:10.1038/353407a0.

Ip, W.-H., and D. A. Mendis (1978), The flute instability as the trigger mechanism for disruption of cometary plasma tails, *Astrophys. J.*, *223*, 671–673, doi:10.1086/156300.

Jia, Y. D., C. T. Russell, L. K. Jian, W. B. Manchester, O. Cohen, A. Vourlidas, K. C. Hansen, M. R. Combi, and T. I. Gombosi (2009), Study of the April 20, 2007 CME—Comet interaction event with an mhd model, *Astrophys. J.*, *696*, L56–L60, doi:10.1088/0004-637X/696/1/L56.

Körösmezey, A., T. E. Cravens, T. I. Gombosi, A. F. Nagy, D. A. Mendis, K. Szegő, B. E. Gribov, R. Z. Sagdeev, V. D. Shapiro, and V. I. Shevchenko (1987), A new model of cometary ionospheres, *J. Geophys. Res.*, *92*, 7331–7340, doi: 10.1029/JA092iA07p07331.

Laroussi, M., G. S. Sayler, B. B. Glascock, B. McCurdy, M. E. Pearce, N. G. Bright, and C. M. Malott (1999), Images of biological samples undergoing sterilization by a glow discharge at atmospheric pressure, *IEEE Trans. Plasma Sci.*, *27*, 34–35, doi: 10.1109/27.763016.

Laroussi, M., D. A. Mendis, and M. Rosenberg (2003), Plasma interaction with microbes, *New J. Phys.*, *5*, 41, doi: 10.1088/1367-2630/5/1/341.

Larson, S. M., and Z. Sekanina (1984), Coma morphology and dust-emission pattern of periodic Comet Halley. I—High-resolution images taken at Mount Wilson in 1910, *Astron. J.*, *89*, 571–578, doi:10.1086/113551.

Manka, R. H. (1973), Plasma and potential at the lunar surface, in *Photon and Particle Interactions in Space*, edited by Grard, R. J. L., D. Reidel, Dordrecht, Netherlands, pp. 347–361.

Marconi, M. L., and D. A. Mendis (1983), The atmosphere of a dirty-clathrate cometary nucleus—A two-phase, multi-fluid model, *Astrophys. J.*, *273*, 381–396, doi:10.1086/161377.

Matsoukas, T., and M. Russell (1995), Particle charging in low-pressure plasmas, *J. Appl. Phys.*, *77*, 4285–4292, doi: 10.1063/1.359451.

Mendis, D. A. (1988), A post-encounter view of comets, *Ann. Rev. Astron. Astrophys*, *26*, 11–49, doi:10.1146/annurev.aa.26.090188.000303.

Mendis, D. A. (2002), Progress in the study of dusty plasmas, *Plasma Sources Sci. Technol.*, *11*(26), A219–228

Mendis, D. A. (2006), The role of comet tails in the discovery of the solar wind and its spatial and temporal variations, in *Recurrent Magnetic Storms: Corotating Solar Wind, American Geophysical Union Geophysical Monograph Series*, edited by R. McPherron, W. Gonzalez, G Lu, H. A. José, and S. Natchimuthukonar Gopalswamy, vol. 167, Am. Geophys. Union Press, Washington, DC, p. 31.

Mendis, D. A. (2007), Solar-comet interactions, in *Handbook of the Solar-Terrestrial Environment*, edited by Y. Kamide, and A. Chian, Springer, Berlin/NY, pp. 494–514.

Mendis, D. A., and M. Rosenberg (1994), Cosmic dusty plasmas, *Annu. Rev. Astron Astr.*, *32*, 419–463, doi:10.1146/annurev.aa.32.090194.002223.

Mendis, D. A., J. R. Hill, H. L. F. Houpis, and E. C. Whipple (1981), On the electrostatic charging of the cometary nucleus, *Astrophys. J.*, *249*, 787–797, doi:10.1086/159337.

Mendis, D. A., H. L. F. Houpis, and M. L. Marconi (1985), The physics of comets, *Fund. Mod. Phys.*, *10*, 1–380.

Mendis, D. A., M. Rosenberg, and F. Azam (2000), A note on the possible electrostatic disruption of bacteria, *IEEE Trans. Plasma Sci.*, *28*, 1304–1306, doi:10.1109/27.893321.

Meyer-Vernet, N (1982), Flip-flop of electric potential of dust grains in space, *Astron. Astrophys.*, *105*, 98–106.

Mitchell, C. J., M. Horányi, O. Havnes, and C. C. Porco (2006), Saturn's apokes: Lost and found, *Science*, *311*, 1587–1589, doi: 10.1126/science.1123783.

Morooka, M. W., J.-E. Wahlund, A. I. Eriksson, W. M. Farrell, D. A. Gurnett, W. S. Kurth, A. M. Persoon, M. Shafiq, M. André, and M. K. G. Holmberg (2011), Dusty plasma in the vicinity of Enceladus, *J. Geophys. Res. Space Phys.*, *116*(A15), A12221, doi: 10.1029/2011JA017038.

Niedner, Jr., M. B., and J. C. Brandt (1978), Interplanetary gas. XXII - Plasma tail disconnection events in comets—

Evidence for magnetic field line reconnection at interplanetary sector boundaries, *Astrophys. J.*, *223*, 655–670, doi:10.1086/156299.

Nitter, T., and O. Havnes (1992), Dynamics of dust in a plasma sheath and injection of dust into the plasma sheath above moon and asteroidal surfaces, *Earth Moon Planets*, *56*, 7–34, doi:10.1007/BF00054597.

Notni, P. (1966), On the forces acting on charged dust particles in cometary atmospheres, *Mém. Soc. Roy. Sci. Liége*, *5*(12), 379–383.

Öpik, E. J. (1956), Interplanetary dust and terrestrial accretion of meteoric matter, *Irish Astron. J.*, *4*, 84.

Poppe, A., and M. Horányi (2010), Simulations of the photoelectron sheath and dust levitation on the lunar surface, *J. Geophys. Res. Space Phys.*, *115*(A14), A08106, doi:10.1029/2010JA015286.

Rahe, J., B. Donn, and K. Wurm (1969), *Atlas of Cometary Forms*, vol. 198., US Government Printing Office, Washington DC.

Rao, N. N., P. K. Shukla, and M. Y. Yu (1990), Dust-acoustic waves in dusty plasmas, *Planet. Space Sci.*, *38*, 543–546, doi:10.1016/0032-0633(90)90147-I.

Reid, G. C. (1990), Ice particles and electron 'bite-outs' at the summer polar mesopause, *J. Geophys. Res.*, *95*, 13,891–13,896, doi:10.1029/JD095iD09p13891.

Reme, H., et al. (1986), Comet Halley-solar wind interaction from electron measurements aboard Giotto, *Nature*, *321*, 349–352, doi:10.1038/321349a0.

Richardson, J. D., and E. C. Sittler, Jr (1990), A plasma density model for Saturn based on Voyager observations, *J. Geophys. Res.*, *95*, 12,019–12,031, doi:10.1029/JA095iA08p12019.

Rosenberg, M (1993), Ion- and dust-acoustic instabilities in dusty plasmas, *Plan. Space Sci.*, *41*, 229–233, doi:10.1016/0032-0633(93)90062-7.

Sagdeev, R. Z., E. N. Evlanov, M. N. Fomenkova, O. F. Prilutskii, and B. V. Zubkov (1989), Small-size dust particles near Halley's Comet, *Adv. Space Res.*, *9*, 263–267, doi:10.1016/0273-1177(89)90272-X.

Schulz, R (2009), Rosetta—One comet rendezvous and two asteroid fly-bys, *Sol. Syst. Res.*, *43*, 343–352, doi:10.1134/S0038094609040091.

Schulz, R., H. Sierks, M. Küppers, and A. Accomazzo (2012), Rosetta fly-by at asteroid (21) Lutetia: An overview, *Planet. Space Sci.*, *66*(1), 2–8, doi:10.1016/j.pss.2011.11.013.

Schwenn, R., W. H. Ip, H. Rosenbauer, H. Balsiger, F. Buhler, R. Goldstein, A. Meier, and E. G. Shelley (1987), Ion temperature and flow profiles in Comet p/ Halley's close environment, *Astron. Astrophys.*, *187*, 160.

Sekanina, Z (1976), *Progress in our understanding of cometary dust trails*, 893–939., vol. 393, US Government Printing Office, Washington DC.

Sekanina, Z. (1987a), Anisotropic emission from comets: Fans versus jets. 1. Concept and modeling, in *Diversity and Similarity of Comets, ESA Special Publication*, edited by E. J. Rolfe, and B. Battrick, vol. 278, ESA Pub. Division, ESTEC, Nordwijk, Netherlands, pp. 315–322.

Sekanina, Z (1987b), Anisotropic emission from comets: Fans versus jets. 2. Periodic Comet Tempel 2, in *Diversity and Similarity of Comets, ESA Special Publication*, vol. 278, ESA Pub. Division, ESTEC, Nordwijk, Netherlands, pp. 323–336.

Sekanina, Z., and P. W. Chodas (2012), Comet C/2011 W3 (Lovejoy): Orbit determination, outbursts, disintegration of nucleus, dust-tail morphology, and relationship to new cluster of bright sungrazers, *Astrophys. J.*, *757*, 127, doi:10.1088/0004-637X/757/2/127.

Sekanina, Z., and J. A. Farrell (1980), The striated dust tail of Comet West VI as a particle fragmentation phenomenon, *Astron. J.*, *85*, 1538–1554, doi:10.1086/112831.

Sekanina, Z., and S. M. Larson (1984), Coma morphology and dust-emission pattern of periodic Comet Halley. II - Nucleus spin vector and modeling of major dust features in 1910, *Astron. J.*, *89*, 1408–1425, doi:10.1086/113643.

Sheridan, T. E., J. Goree, Y. T. Chiu, R. L. Rairden, and J. A. Kiessling (1992), Observation of dust shedding from material bodies in a plasma, *J. Geophys. Res.*, *97*, 2935–2942, doi:10.1029/91JA02801.

Shukla, P., and A. Mamun (2002), *Introduction to the Physics of Dusty Plasmas*, IOP Series in Plasma Physics, Inst. of Phys. Pub., Bristol and Philadelphia.

Shukla, P. K., and V. P. Silin (1992), Dust ion-acoustic wave, *Phys. Scr.*, *45*, 508, doi:10.1088/0031-8949/45/5/015.

Sickafoose, A. A., J. E. Colwell, M. Horányi, and S. Robertson (2002), Experimental levitation of dust grains in a plasma sheath, *J. Geophys. Res. A: Space Phys.*, *107*, 1408, doi:10.1029/2002JA009347.

Simpson, J. A., D. Rabinowitz, A. J. Tuzzolino, L. V. Ksanfomaliti, and R. Z. Sagdeev (1987), The dust coma of comet P/Halley - Measurements on the Vega-1 and Vega-2 spacecraft, *Astron. Astrophys.*, *187*, 742–752.

Singer, S. F., and E. H. Walker (1962), Electrostatic dust transport on the lunar surface, *Icarus*, *1*, 112, doi:10.1016/0019-1035(62)90011-8.

Thompson, C., A. Barkan, R. L. Merlino, and N. D'Angelo (1999), Video imaging of dust acoustic waves, *IEEE Trans. Plasma Sci.*, *27*, 146–147, doi:10.1109/27.763096.

Tsurutani, B. T., D. R. Clay, L. D. Zhang, B. Dasgupta, D. Brinza, M. Henry, J. K. Arballo, S. Moses, and A. Mendis (2004), Plasma clouds associated with Comet P/Borrelly dust impacts, *Icarus*, *167*, 89–99, doi:10.1016/j.icarus.2003.08.021.

Tsytovich, V., G. Morfill, S. Vladimirov, and H. Thomas (2008), *Elementary Physics of Complex Plasmas*, 370 pp., (Lecture Notes in Physics), vol. 731, Springer Berlin, Heidelberg.

Verheest, F. (ed.) (2000), *Waves in Dusty Space Plasmas, Astrophysics and Space Science Library*, vol. 245, Kluwer Acad. Pub., Dordrecht, Netherlands.

Walch, B., M. Horányi, and S. Robertson (1995), Charging of dust grains in plasma with energetic electrons, *Phys. Rev. Lett.*, *75*, 838–841, doi:10.1103/PhysRevLett.75.838.

Wallis, M. K., and M. H. A. Hassan (1983), Electrodynamics of submicron dust in the cometary coma, *Astron. Astrophys.*, *121*, 10–14

Wallis, M. K., and R. S. B. Ong (1975), Strongly-cooled ionizing plasma flows with application to Venus, *Planet. Space Sci.*, *23*, 713–721, doi:10.1016/0032-0633(75)90109-9.

Wang, X., M. Horányi, Z. Sternovsky, S. Robertson, and G. E. Morfill (2007), A laboratory model of the lunar surface potential near boundaries between sunlit and shadowed regions, *Geophys. Res. Lett.*, *34*, L16104, doi:10.1029/2007GL030766.

Wang, X., M. Horányi, and S. Robertson (2009), Experiments on dust transport in plasma to investigate the origin of the lunar horizon glow, *J. Geophys. Res. A: Space Phys.*, *114*(A13), A05103, doi:10.1029/2008JA013983.

Watanabe, Y. (1997), Dust phenomena in processing plasmas, *Plasma Phys. Controlled Fusion*, *39*(5A), A59

Weaver, H. A. (2004), Not a rubble pile? *Science*, *304*, 1760–1761

Whipple, E. C. (1981), Potentials of surfaces in space, *Rep. Prog. Phys.*, *44*, 1197–1250, doi:10.1088/0034-4885/44/11/002.

Whipple, E. C., T. G. Northrop, and D. A. Mendis (1985), The electrostatics of a dusty plasma, *J. Geophys. Res.*, *90*, 7405–7413, doi:10.1029/JA090iA08p07405.

Whipple, F. L. (1950), A comet model. I. The acceleration of Comet Encke, *Astrophys. J.*, *111*, 375–394, doi:10.1086/145272.

Winske, D., S. P. Gary, M. E. Jones, M. Rosenberg, V. W. Chow, and D. A. Mendis (1995), Ion heating in a dusty plasma due to the dust/ion acoustic instability, *Geophys. Res. Lett.*, *22*, 2069–2072, doi:10.1029/95GL01983.

Xu, W., N. D'Angelo, and R. L. Merlino (1993), Dusty plasmas - The effect of closely packed grains, *J. Geophys. Res.*, *98*, 7843–7847, doi:10.1029/93JA00309.